International Journal of Development Mathematics Vol 3 Issue 1, 001-042

INTERNATIONAL JOURNAL OF DEVELOPMENT MATHEMATICS

ISSN: 3026-8656 (Print) | 3026-8699 (Online)

journal homepage: https://ijdm.org.ng/index.php/Journals

Mathematical Modelling of East Coast Fever and Foot-and-Mouth Disease Co-Infection in Cattle in Malawi

David Nyirenda[a*], Patrick Phepa[b], Nelson Dzupire[c], Patrick Chidzalo[d]

[a]Biomedical Engineering Department, Malawi Institute of Technology, Malawi University of Science and Technology, Thyolo, Malawi.

[b]Mathematical Sciences Department, School of Science and Technology, Malawi University of Business and Applied Sciences, Blantyre, Malawi.

[c]Mathematical Sciences Department, School of Applied and Natural Sciences, University of Malawi, Zomba, Malawi.

[d]Applied Studies Department, Malawi Institute of Technology, Malawi University of Science and Technology, Thyolo, Malawi.

ARTICLE INFO

Article history:
Received 30 December 2025
Received in Revised 20 February 2026
Accepted 25 February 2026

Keywords
Cattle diseases, East Coast Fever, Foot-and-Mouth Disease, Co-infection, Epidemiological modelling, Mathematical model.

MSC 2020 Subject classification: 92D30, 92C60, 49K15.

*Corresponding author Tel:+265991270374
Email address: bme-032-17@must.ac.mw
https://doi.org/10.62054/ijdm/0301.01

Abstract

This study develops a mathematical model to describe the co-infection dynamics of East Coast Fever (ECF) and Foot-and-Mouth Disease (FMD) in cattle, with a focus on livestock production systems in Malawi. The model accounts for direct transmission of FMD among cattle and tick-mediated transmission of ECF, allowing for progression from single infection to co-infection. Threshold quantities in the form of basic reproduction numbers are derived to analyze the stability of disease-free and endemic equilibria. Sensitivity analysis indicates that ECF transmission is strongly influenced by tick mortality and vector-to-cattle transmission, while FMD

dynamics are primarily driven by cattle recruitment and direct contact rates. An optimal control framework incorporating vaccination, treatment, and vector control is formulated to assess the effectiveness of intervention strategies. Numerical simulations, using parameter values relevant to Malawian cattle farming, show that the disease-free equilibrium is unstable under baseline conditions, reflecting the endemicity of ECF and the recurring nature of FMD outbreaks. However, combined intervention strategies substantially reduce infection prevalence and can eliminate both diseases. These findings highlight the importance of integrated control measures targeting both cattle and tick populations and provide a quantitative framework to support improved management of ECF-FMD co-infection in Malawi.

1 Introduction

Cattle farming is a cornerstone of agricultural production in developing countries, contributing significantly to household livelihoods, food security, and the national economy (Banda & Tanganyika, 2021; Herrero *et al.*, 2009; Herrero *et al.*, 2013). As a developing country, the country relies heavily on traditional cattle management practices, predominantly involving indigenous Malawi Zebu cattle, which account for over 90% of the national herd, while exotic and crossbred animals make up the remaining 8–10% (Chatanga *et al.*, 2022). Cattle are raised both for beef production and for dairy purposes, providing essential protein sources and income for smallholder farmers (Sibanda, 2014). The economic and social importance of cattle underscores the need for effective disease management, particularly in contexts where veterinary infrastructure and resources are limited.

Livestock in Malawi, and more broadly Sub-Saharan Africa, is susceptible to numerous infectious diseases, many of which are transmitted by arthropod vectors such as ticks (Minjauw & McLeod, 2003; Monakale *et al.*, 2024; Djiman *et al.*, 2024). Among these, East Coast Fever (ECF), caused by *Theileria parva* and transmitted by *Rhipicephalus appendiculatus*, and Foot-and-Mouth Disease (FMD), caused by an Aphthovirus, stand out as two of the most economically and epidemiologically significant diseases (Keeling, 2005; Mumba *et al.*, 2017). ECF is a protozoan infection that can result in high morbidity and mortality, particularly in naïve or crossbred cattle, and has been shown to exert complex dynamics between host immunity, tick vectors, and pathogen persistence. FMD, on the other hand, is a highly contagious viral disease that affects multiple cloven-hoofed species, leading to production losses, trade restrictions, and severe economic impacts (Wongnak *et al.*, 2024; Shikumwifa, 2022).

While numerous studies have explored ECF and FMD individually, limited attention has been given to their potential co-infections in cattle. Co-infections of a host by multiple pathogens are increasingly recognized as a critical factor shaping disease dynamics, severity, and transmission. In human epidemiology, mathematical models have been developed to quantify interactions between viral and bacterial pathogens, investigating whether co-infections enhance susceptibility, alter infectiousness or mortality, and affect the overall spread of disease (Inayaturohmat *et al.*, 2024). Adopting this framework for livestock can

provide insights into the synergistic or antagonistic effects of ECF and FMD co-infections and inform evidence-based disease management strategies in Malawi.

Existing epidemiological models for ECF and FMD typically employ compartmental frameworks such as SIR, SEIR, or SIRS models, incorporating host-vector interactions, pathogen transmission rates, and population demographics (Gilioli *et al.*, 2009; Fahcruddin *et al.*, 2023). These models have demonstrated the utility of threshold conditions, endemic stability concepts, and intervention simulations to identify critical control strategies (Pesciaroli *et al.*, 2025). However, translating these approaches to co-infection scenarios presents additional challenges, including parameter interdependencies, altered transmission or mortality rates, and the need for multi-pathogen data inputs. Robust co-infection models must integrate realistic assumptions, epidemiological parameters, and control measures to produce actionable predictions for disease mitigation (Yano *et al.*, 2024).

In this study, we aim to bridge this gap by developing a mathematical model for ECF and FMD co-infections in Malawian cattle, reflecting both traditional and modern cattle-keeping practices. Specifically, the study addresses the following objectives:

1. Develop a compartmental model capturing the dynamics of ECF and FMD co-infections in cattle, accounting for pathogen interactions, vector dynamics, and host demographics.

2. Investigate how co-infections influence susceptibility, disease severity, mortality, and transmission potential.

3. Explore the impact of control strategies, such as vaccination and vector management, on the epidemiological outcomes of co-infected populations.

By synthesizing principles from human co-infection modeling (Yano *et al.*, 2024) and existing ECF and FMD research (Gilioli *et al.*, 2009; Pesciaroli *et al.*,2025; Shikumwifa, 2022), this study provides a conceptual and quantitative framework for understanding and managing co-infections in Malawian cattle. The findings are expected to inform policy, improve disease control interventions, and enhance livestock productivity, contributing to both local livelihoods and national economic development.
The remainder of the paper is organized as follows: Section 2 presents the mathematical formulation of the co-infection model and perform theoretical analyses, including equilibrium points and stability conditions. In Section 3 we formulate an optimal control problem; Section 4 is two folds: it first illustrates numerical simulations, and then discusses implications for disease management and control; finally, Section 5 concludes with key findings and recommendations for future work.

2 Mathematical Model Formulation

This section presents the formulation of a deterministic compartmental model describing the co-infection dynamics of East Coast Fever (ECF) and Foot-and-Mouth Disease (FMD) in cattle, incorporating tick (vector) transmission for ECF and direct cattle-to-cattle transmission for FMD. The model builds upon standard host–vector epidemic frameworks, adapted

from multi-pathogen co-infection structures developed in human epidemiology (Inayaturohmat *et al.*, 2024), but tailored here to the biological and ecological context of Malawian cattle.

2.1 Model assumptions and population structure

The total cattle population at time t, denoted by $N_c(t)$, is divided into five mutually exclusive compartments:

$$N_c(t) = S(t) + I_e(t) + I_f(t) + I_{ef}(t) + R(t),$$

where:

- $S(t)$: susceptible cattle that are free from both ECF and FMD;
- $I_e(t)$: cattle infected only with ECF;
- $I_f(t)$: cattle infected only with FMD;
- $I_{ef}(t)$: cattle co-infected with both ECF and FMD;
- $R(t)$: cattle that have recovered from one or both infections and are temporarily immune.

Similarly, the total tick population at time t, denoted by $N_v(t)$, is divided into two compartments:

$$N_v(t) = S_v(t) + I_v(t),$$

where $S_v(t)$ represents susceptible ticks and $I_v(t)$ represents ECF-infectious ticks capable of transmitting the disease to cattle.

The following biological assumptions are made:

1. Recruitment of susceptible cattle and ticks occurs at constant rates Λ_c and Λ_v, respectively.
2. Natural deaths occur at rates μ_c for cattle and μ_v for ticks.
3. ECF transmission occurs when susceptible cattle are bitten by infected ticks, at rate $\beta_e S I_v$.
4. Ticks acquire infection when they feed on infected cattle (I_e or I_{ef}) at rate $\alpha_v S_v(I_e + I_{ef})$.
5. FMD spreads directly through contact between infectious and susceptible cattle, at rate $\beta_f S I_f$.
6. Co-infection can arise in two ways: ECF-infected cattle acquiring FMD at rate $\eta_{ef} I_e$, and FMD-infected cattle acquiring ECF at rate $\eta_{fe} I_f$.
7. Recovery rates from ECF, FMD, and co-infection are denoted by γ_e, γ_f, and γ_{ef}, respectively.

The mathematical model describing the co-infection dynamics of East Coast Fever (ECF) and Foot-and-Mouth Disease (FMD) involves seven interconnected compartmental variables across two populations: cattle (N_c) and ticks (N_v).

The cattle population is divided into five compartments: Susceptible (S), ECF-infected (I_e), FMD-infected (I_f), Co-infected (I_{ef}), and Recovered (R). The tick population is divided into two compartments: Susceptible ticks (S_v) and ECF-infectious ticks (I_v).

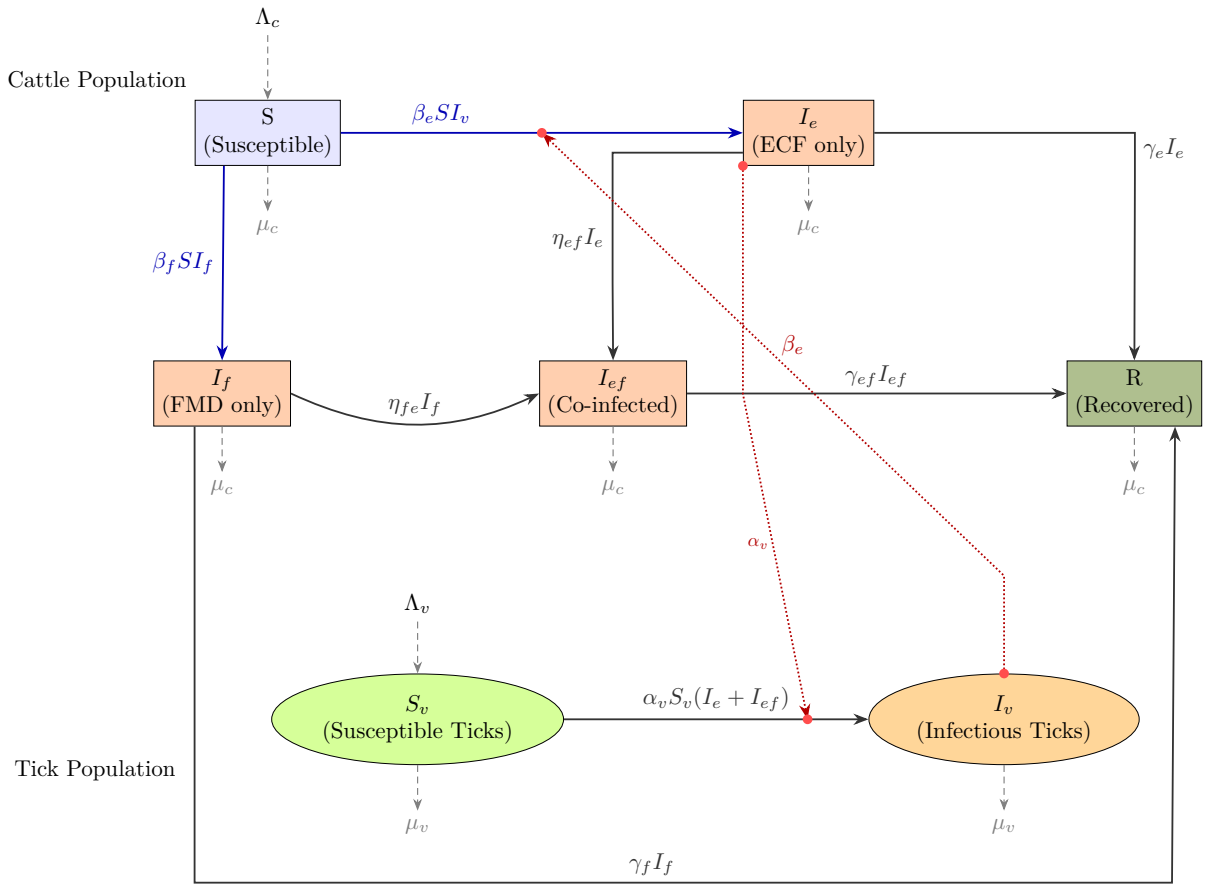

Figure 1: FMD/ECF co-infection model diagram.

2.2 Model equations

Under these assumptions, the transmission dynamics of ECF and FMD in cattle and ticks are governed by the following system of ordinary differential equations:

$$
\begin{aligned}
\dot{S} &= \Lambda_c - \beta_e S I_v - \beta_f S I_f - \mu_c S, \\
\dot{I}_e &= \beta_e S I_v - (\eta_{ef} + \gamma_e + \mu_c) I_e, \\
\dot{I}_f &= \beta_f S I_f - (\eta_{fe} + \gamma_f + \mu_c) I_f, \\
\dot{I}_{ef} &= \eta_{ef} I_e + \eta_{fe} I_f - (\gamma_{ef} + \mu_c) I_{ef}, \\
\dot{R} &= \gamma_e I_e + \gamma_f I_f + \gamma_{ef} I_{ef} - \mu_c R, \\
\dot{S}_v &= \Lambda_v - \alpha_v S_v (I_e + I_{ef}) - \mu_v S_v, \\
\dot{I}_v &= \alpha_v S_v (I_e + I_{ef}) - \mu_v I_v.
\end{aligned} \tag{1}
$$

Equation set (1) captures the biological and epidemiological interactions between cattle and ticks, as well as the transition pathways for single and double infections. The first five equations describe cattle dynamics, while the last two represent the tick population. Figure 1 shows the model diagram defining the system (1).

The infection process proceeds as follows: susceptible cattle become infected with ECF when bitten by infectious ticks (I_v); ECF-infected cattle can then recover, die naturally, or acquire FMD to move into the co-infected compartment. Similarly, FMD-infected cattle may recover, die, or acquire ECF through tick bites. Ticks acquire ECF by feeding on infected cattle and remain infectious until death.

Before proceeding we state that Tables 1 and 2 summarize the state variables and parameters used in the model formulation.

Variable	**Description**
S	Susceptible cattle population
I_e	Cattle infected only with ECF
I_f	Cattle infected only with FMD
I_{ef}	Cattle co-infected with ECF and FMD
R	Recovered cattle population
S_v	Susceptible tick population
I_v	Infected ticks transmitting ECF
N_c	Total cattle population: $S + I_e + I_f + I_{ef} + R$
N_v	Total tick population: $S_v + I_v$

Table 1: State variables for the ECF–FMD co-infection model.

2.3 Qualitative Analysis of the FMD Model

To begin our analysis, we consider the FMD-only dynamics by setting all ECF-related terms and co-infection compartments to zero:

$$I_e = I_{ef} = S_v = I_v = 0.$$

Parameter	Description	Units
Λ_c	Recruitment rate of cattle	heads/day
Λ_v	Recruitment rate of ticks	ticks/day
μ_c	Natural death rate of cattle	day^{-1}
μ_v	Natural death rate of ticks	day^{-1}
β_e	Transmission rate of ECF from ticks to cattle	day^{-1}
β_f	Transmission rate of FMD from cattle to cattle	day^{-1}
α_v	Transmission rate of ECF from cattle to ticks	day^{-1}
γ_e	Recovery rate from ECF	day^{-1}
γ_f	Recovery rate from FMD	day^{-1}
γ_{ef}	Recovery rate from co-infection	day^{-1}
η_{ef}	Rate at which ECF-infected cattle acquire FMD	day^{-1}
η_{fe}	Rate at which FMD-infected cattle acquire ECF	day^{-1}

Table 2: Model parameters and their biological meanings.

This reduces System (1) to a simplified three-compartment model describing FMD in cattle:

$$\begin{aligned} \dot{S} &= \Lambda_c - \beta_f S I_f - \mu_c S, \\ \dot{I}_f &= \beta_f S I_f - (\gamma_f + \mu_c) I_f, \\ \dot{R} &= \gamma_f I_f - \mu_c R. \end{aligned} \tag{2}$$

2.4 Basic properties of the FMD-only model

To verify the well-posedness of the FMD-only model (2), we investigate the positivity and boundedness of its solutions.

2.4.1 Positivity of the solutions

The FMD-only system (2) describes the dynamics of susceptible, infected, and recovered cattle populations. The model will therefore be biologically meaningful in the feasible region Ω when all state variables remain positive for all $t \geq 0$.

Theorem 2.1 (Positivity of solutions)**.** *Let the initial condition be* $\{S(0), I_f(0), R(0) \geq 0\} \in \Omega$. *Then the solution set* $\{S(t), I_f(t), R(t)\}$ *of the system* (2) *is positive for all* $t > 0$.

Proof. Consider the first equation of the system (2):

$$\frac{dS}{dt} = \Lambda_c - \beta_f S I_f - \mu_c S \tag{3}$$

It is clear from (3) that

$$\frac{dS}{dt} \geq -(\beta_f I_f + \mu_c) S$$

Integrating both sides using separation of variables gives:

$$\int \frac{dS}{S} \geq -\int (\beta_f I_f + \mu_c)dt$$

which leads to

$$S(t) \geq S(0)e^{-(\beta_f I_f + \mu_c)t} \geq 0 \tag{4}$$

Thus, $S(t) \geq 0$ for all $t \geq 0$.

Similarly, for the infected compartment:

$$\frac{dI_f}{dt} = \beta_f S I_f - (\gamma_f + \mu_c)I_f \geq -(\gamma_f + \mu_c)I_f \tag{5}$$

Separating variables and integrating gives

$$I_f(t) \geq I_f(0)e^{-(\gamma_f + \mu_c)t} \geq 0 \tag{6}$$

Thus, $I_f(t) \geq 0$ for all $t \geq 0$.

For the recovered compartment:

$$\frac{dR}{dt} = \gamma_f I_f - \mu_c R \geq -\mu_c R \tag{7}$$

Integrating gives

$$R(t) \geq R(0)e^{-\mu_c t} \geq 0 \tag{8}$$

Hence, $R(t) \geq 0$ for all $t \geq 0$.

Therefore, all state variables remain non-negative:

$$S(t) \geq 0, \quad I_f(t) \geq 0, \quad R(t) \geq 0, \quad \forall t \geq 0.$$

□

2.4.2 Boundedness of the solution

We now show that the total cattle population

$$N_c(t) = S(t) + I_f(t) + R(t)$$

remains within biologically realistic bounds.

Theorem 2.2 (Boundedness of solutions)**.** *The solutions of the FMD-only system* (2) *are contained in the feasible region*

$$\Omega = \{S, I_f, R \geq 0 : N_c \leq \frac{\Lambda_c}{\mu_c}\}.$$

Proof. Taking the derivative of the total population $N_c(t)$:

$$\begin{aligned}\frac{dN_c}{dt} &= \frac{dS}{dt} + \frac{dI_f}{dt} + \frac{dR}{dt} \\ &= \Lambda_c - \beta_f S I_f - \mu_c S + \beta_f S I_f - (\gamma_f + \mu_c) I_f + \gamma_f I_f - \mu_c R \\ &= \Lambda_c - \mu_c (S + I_f + R) \\ &= \Lambda_c - \mu_c N_c\end{aligned}$$

Thus,

$$\frac{dN_c}{dt} + \mu_c N_c = \Lambda_c$$

Of course we require that

$$\frac{dN_c}{dt} + \mu_c N_c \leq \Lambda_c$$

Solving this differential inequality using the integration factor method gives:

$$N_c(t) \leq \frac{\Lambda_c}{\mu_c} + \left(N_c(0) - \frac{\Lambda_c}{\mu_c} \right) e^{-\mu_c t}$$

Taking the limit as $t \to \infty$:

$$0 \leq \lim_{t \to \infty} N_c(t) \leq \frac{\Lambda_c}{\mu_c}$$

Hence, the total population remains bounded in the feasible region

$$\Omega = \{S, I_f, R \geq 0 : N_c \leq \Lambda_c / \mu_c\}.$$

□

Our analysis demonstrates the positivity and boundedness of solutions to the FMD-only system. Positivity ensures non-negative populations, while boundedness ensures that the total cattle population remains within realistic biological limits (Hethcote, 2000).

The disease-free equilibrium (DFE) of (2) corresponds to the state with no infection, i.e.,

$$\mathbf{E}_{f0} = \left(S^*, I_f^*, R^* \right) = \left(\frac{\Lambda_c}{\mu_c}, 0, 0 \right). \tag{9}$$

2.4.3 Basic Reproduction Number

To rigorously compute the basic reproduction number of FMD, we use the next-generation operator method (van denDriessche and Watmough, 2002). Let $\mathbf{x} = I_f$ denote the infectious compartment. We define:

- $\mathcal{F}(\mathbf{x})$ as the rate of appearance of new infections in compartment I_f,
- $\mathcal{V}(\mathbf{x})$ as the rate of transfer out of the infectious compartment (including recovery and natural death).

For Model (2), the disease-free equilibrium (DFE) occurs when there are no infected individuals, $I_f = 0$. Solving the system under this condition gives

$$E_{f0} = \left(\frac{\Lambda_c}{\mu_c}, 0, 0\right), \tag{10}$$

where the susceptible population is at $S^* = \Lambda_c/\mu_c$ and the recovered population is $R^* = 0$.

To assess the local stability of this equilibrium with respect to disease invasion, we compute the basic reproduction number R_0 using the next-generation matrix approach.

Following the standard procedure, we separate the dynamics into new infection terms F and other transition terms V for the infected compartment I_f:

$$F = \frac{\partial(\beta_f S I_f)}{\partial I_f}\Big|_{E_0} = \beta_f S^* = \beta_f \frac{\Lambda_c}{\mu_c}, \quad V = \frac{\partial((\gamma_f + \mu_c) I_f)}{\partial I_f}\Big|_{E_0} = \gamma_f + \mu_c. \tag{11}$$

The next-generation matrix is simply

$$K = FV^{-1}, \tag{12}$$

and thus the basic reproduction number is the spectral radius of K:

$$\mathcal{R}_{f0} = \rho(K) = \frac{\beta_f \Lambda_c}{\mu_c(\gamma_f + \mu_c)}. \tag{13}$$

This quantity represents the expected number of secondary infections produced by a single infected cattle introduced into a fully cattle susceptible population.

2.4.4 Local stability of the disease-free equilibrium

Theorem 2.3 (Local asymptotic stability of the DFE)**.** *The disease-free equilibrium* $E_{f0} = \left(\frac{\Lambda_c}{\mu_c}, 0, 0\right)$ *of the FMD model* (2) *is locally asymptotically stable if* $\mathcal{R}_{f0} < 1$ *and unstable if* $\mathcal{R}_{f0} > 1$.

Proof. To investigate local stability, we first compute the Jacobian matrix of system (2) in terms of partial derivatives:

$$\mathcal{J}(S, I_f, R) = \begin{pmatrix} \frac{\partial \dot{S}}{\partial S} & \frac{\partial \dot{S}}{\partial I_f} & \frac{\partial \dot{S}}{\partial R} \\ \frac{\partial \dot{I}_f}{\partial S} & \frac{\partial \dot{I}_f}{\partial I_f} & \frac{\partial \dot{I}_f}{\partial R} \\ \frac{\partial \dot{R}}{\partial S} & \frac{\partial \dot{R}}{\partial I_f} & \frac{\partial \dot{R}}{\partial R} \end{pmatrix}. \tag{14}$$

From (2), the partial derivatives are

$$\begin{aligned} &\frac{\partial \dot{S}}{\partial S} = -\beta_f I_f - \mu_c, && \frac{\partial \dot{S}}{\partial I_f} = -\beta_f S, && \frac{\partial \dot{S}}{\partial R} = 0, \\ &\frac{\partial \dot{I}_f}{\partial S} = \beta_f I_f, && \frac{\partial \dot{I}_f}{\partial I_f} = \beta_f S - (\gamma_f + \mu_c), && \frac{\partial \dot{I}_f}{\partial R} = 0, \\ &\frac{\partial \dot{R}}{\partial S} = 0, && \frac{\partial \dot{R}}{\partial I_f} = \gamma_f, && \frac{\partial \dot{R}}{\partial R} = -\mu_c. \end{aligned}$$

Next, evaluating (14) at the disease-free equilibrium $E_0 = (\Lambda_c/\mu_c, 0, 0)$ yields

$$\mathcal{J}_0 = \begin{pmatrix} -\mu_c & -\beta_f \frac{\Lambda_c}{\mu_c} & 0 \\ 0 & \beta_f \frac{\Lambda_c}{\mu_c} - (\gamma_f + \mu_c) & 0 \\ 0 & \gamma_f & -\mu_c \end{pmatrix}. \tag{15}$$

We determine the eigenvalues of the matrix in (15) by solving the characteristic equation

$$\det\left(\mathcal{J}_0 - \lambda I_{3\times 3}\right) = 0 \tag{16}$$

where $I_{3\times 3}$ is the 3×3 identity matrix and λ represents the eigenvalues.

The eigenvalues of $\mathcal{J}_0$ are obtained by noting that it is upper block-triangular. Clearly,

$$\lambda_1 = \lambda_2 = -\mu_c,$$

and the remaining eigenvalue is

$$\begin{aligned} \lambda_3 &= \frac{\Lambda_c \beta_f - \gamma_f \mu_c - \mu_c^2}{\mu_c} \\ &= \beta_f \frac{\Lambda_c}{\mu_c} - (\gamma_f + \mu_c) \\ &= (\gamma_f + \mu_c)(\mathcal{R}_{f0} - 1), \end{aligned}$$

where the basic reproduction number $\mathcal{R}_{f0}$ of the FMD model is given by (17)

$$\mathcal{R}_{f0} = \frac{\beta_f \Lambda_c}{\mu_c(\gamma_f + \mu_c)}. \tag{17}$$

Hence, if $\mathcal{R}_{f0} < 1$, all eigenvalues of $\mathcal{J}_0$ have negative real parts and the DFE is locally asymptotically stable. Conversely, if $\mathcal{R}_{f0} > 1$, the DFE is unstable. □

Remark 2.4. *At this point, we comment that*

1. *The basic reproduction number $\mathcal{R}_{f0}$ represents the expected number of secondary FMD cases generated by a single infected animal in a fully susceptible cattle population.*
2. *If $\mathcal{R}_{f0} < 1$, the infection will eventually die out, whereas if $\mathcal{R}_{f0} > 1$, FMD can invade the population and persist.*

2.4.5 Endemic equilibrium of the FMD-only model

The endemic equilibrium corresponds to the persistent presence of FMD in the cattle population and is obtained by setting

$$\dot{S} = \dot{I}_f = \dot{R} = 0$$

in system (2), with $I_f^* > 0$.

Let

$$\mathbf{E}_f^* = (S_f^*, I_f^*, R_f^*)$$

denote the endemic equilibrium point. From (2), we obtain the steady-state system (18):

$$\begin{aligned} 0 &= \Lambda_c - \beta_f S^* I_f^* - \mu_c S^* \\ 0 &= \beta_f S^* I_f^* - (\gamma_f + \mu_c) I_f^* \\ 0 &= \gamma_f I_f^* - \mu_c R^* \end{aligned} \tag{18}$$

Since $I_f^* > 0$, we can rewrite the second equation of (18) as

$$\beta_f S_f^* = \gamma_f + \mu_c \quad \Longrightarrow \quad S_f^* = \frac{\gamma_f + \mu_c}{\beta_f}. \tag{19}$$

Substituting (19) in the first equation of (18) gives

$$\begin{aligned} 0 &= \Lambda_c - \beta_f S_f^* I_f^* - \mu_c S_f^* \\ &= \Lambda_c - (\gamma_f + \mu_c) I_f^* - \mu_c \frac{\gamma_f + \mu_c}{\beta_f}. \end{aligned}$$

Solving for I_f^*, we obtain

$$I_f^* = \frac{\Lambda_c}{\gamma_f + \mu_c} \left(1 - \frac{1}{\mathcal{R}_{f0}}\right), \tag{20}$$

where $\mathcal{R}_{f0}$ is defined in (17). Clearly, $I_f^* > 0$ if and only if $\mathcal{R}_{f0} > 1$.

Finally, from the last equation of (18), the recovered population at endemic equilibrium is

$$R_f^* = \frac{\gamma_f}{\mu_c} I_f^* = \frac{\gamma_f}{\mu_c} \frac{\Lambda_c}{\gamma_f + \mu_c} \left(1 - \frac{1}{\mathcal{R}_{f0}}\right). \tag{21}$$

Therefore, the endemic equilibrium of the FMD-only model (2) is given by

$$\mathbf{E}_f^* = \left(\frac{\gamma_f + \mu_c}{\beta_f} \frac{\Lambda_c}{\gamma_f + \mu_c} \left(1 - \frac{1}{\mathcal{R}_{f0}}\right), \frac{\gamma_f}{\mu_c} \frac{\Lambda_c}{\gamma_f + \mu_c} \left(1 - \frac{1}{\mathcal{R}_{f0}}\right) \right), \tag{22}$$

which exists uniquely whenever $\mathcal{R}_{f0} > 1$.

Theorem 2.3 indicates that FMD infection can be contained within the cattle population if the initial numbers of susceptible, infected, and recovered animals lie within the region of attraction of the disease-free equilibrium $\mathbf{E}_{f0}$. To guarantee that disease control does not depend on the initial population distribution, it is therefore necessary to establish the global asymptotic stability of the equilibrium points.

Proposition 2.5. *If $\mathcal{R}_{f0} < 1$, the disease-free equilibrium $\mathbf{E}_{f0}$ of the FMD model (2) is globally asymptotically stable. If $\mathcal{R}_{f0} > 1$, the endemic equilibrium point $\mathbf{E}_f^*$ is global asymptotic stable.*

Proof. We establish the global asymptotic stability of the endemic equilibrium $\mathbf{E}_f^*$ when $\mathcal{R}_{f0} > 1$.

From system (2), note that the third equation is decoupled from the susceptible population S_f. At equilibrium, it satisfies

$$0 = \gamma_f I_f - \mu_c R,$$

which implies

$$R = \frac{\gamma_f}{\mu_c} I_f.$$

Substituting this expression into the first two equations of (2), we obtain the following planar system in (S_f, I_f):

$$\begin{aligned} \frac{dS_f}{dt} &= \Lambda_c - \beta_f S_f I_f - \mu_c S_f, \\ \frac{dI_f}{dt} &= \beta_f S_f I_f - (\gamma_f + \mu_c) I_f. \end{aligned} \tag{23}$$

Standard asymptotic arguments imply that solutions of the full system (2) approach those of the reduced planar system (23) as $t \to \infty$ (Thieme,2003). Therefore, it suffices to study the global dynamics of (23).

Define the positively invariant region

$$\Omega_f = \left\{ (S_f, I_f) \in \mathbb{R}^2_+ : S_f + I_f \leq \frac{\Lambda_c}{\mu_c} \right\}.$$

When $\mathcal{R}_{f0} > 1$, system (23) admits a unique endemic equilibrium $\mathbf{E}^*_f$ in the interior of Ω_f, which is locally asymptotically stable.

To exclude the existence of periodic orbits in Ω_f, we apply the Dulac–Bendixson criterion (Perko, 2001). Let

$$\phi(S_f, I_f) = \frac{1}{S_f I_f}, \quad S_f > 0,\ I_f > 0.$$

Let $\mathbf{\Gamma}(S_f, I_f) = (\theta, \delta)$ denote the vector field of (23), where

$$\theta(S, I) = \Lambda_c - \beta_f S_f I_f - \mu_c S_f, \quad \delta(S, I) = \beta_f S_f I_f - (\gamma_f + \mu_c) I_f.$$

We compute

$$\nabla \cdot (\phi \mathbf{\Gamma}) = \frac{\partial}{\partial S_f}(\phi\theta) + \frac{\partial}{\partial I_f}(\phi\delta).$$

First,

$$\phi\theta = \frac{\Lambda_c}{S_f I_f} - \beta_f - \frac{\mu_c}{I_f},$$

so that

$$\frac{\partial}{\partial S_f}(\phi\theta) = -\frac{\Lambda_c}{S_f^2 I_f}.$$

Next,

$$\phi\delta = \beta_f - \frac{\gamma_f + \mu_c}{S_f},$$

and hence

$$\frac{\partial}{\partial I_f}(\phi\delta) = 0.$$

Therefore,

$$\nabla \cdot (\phi X) = -\frac{\Lambda_c}{S_f^2 I_f} < 0, \quad \text{for all } (S_f, I_f) \in \Omega_f^\circ.$$

By the Dulac–Bendixson criterion, system (23) admits no periodic orbits in Ω_f. Since Ω_f is compact and positively invariant, and $\mathbf{E}_f^*$ is the unique equilibrium in its interior, the Poincaré–Bendixson theorem implies that every trajectory in $\Omega_f \setminus \{\mathbf{E}_{f0}\}$ converges to $\mathbf{E}_f^*$.

Hence, the endemic equilibrium $\mathbf{E}_f^*$ of the FMD-only model (2) is globally asymptotically stable whenever $\mathcal{R}_{f0} > 1$. □

2.5 Qualitative Analysis of the ECF Model

To analyze the ECF-only dynamics, we set all FMD-related terms and compartments to zero:

$$I_f = I_{ef} = 0.$$

The full system (1) then reduces to the host-vector ECF model (24):

$$\begin{aligned} \dot{S} &= \Lambda_c - \beta_e S I_v - \mu_c S \\ \dot{I}_e &= \beta_e S I_v - (\gamma_e + \mu_c) I_e \\ \dot{R} &= \gamma_e I_e - \mu_c R \\ \dot{S}_v &= \Lambda_v - \alpha_v S_v I_e - \mu_v S_v \\ \dot{I}_v &= \alpha_v S_v I_e - \mu_v I_v \end{aligned} \tag{24}$$

2.5.1 Positivity of solutions

Theorem 2.6 (Positivity of solutions)**.** *Let the initial conditions satisfy*

$$S(0), I_e(0), R(0), S_v(0), I_v(0) \geq 0.$$

Then the solutions of system (24) *remain non-negative for all* $t \geq 0$.

Proof. For susceptible cattle:

$$\frac{dS}{dt} = \Lambda_c - \beta_e S I_v - \mu_c S \geq -(\beta_e I_v + \mu_c) S,$$

which implies

$$S(t) \geq S(0) e^{-(\beta_e I_v + \mu_c)t} \geq 0.$$

For infected cattle:

$$\frac{dI_e}{dt} = \beta_e S I_v - (\gamma_e + \mu_c) I_e \geq -(\gamma_e + \mu_c) I_e,$$

so that

$$I_e(t) \geq I_e(0) e^{-(\gamma_e + \mu_c)t} \geq 0.$$

For recovered cattle:

$$\frac{dR}{dt} = \gamma_e I_e - \mu_c R \geq -\mu_c R \implies R(t) \geq R(0) e^{-\mu_c t} \geq 0.$$

For susceptible and infected ticks:

$$\frac{dS_v}{dt} \geq -(\alpha_v I_e + \mu_v) S_v, \quad \frac{dI_v}{dt} \geq -\mu_v I_v \implies S_v(t), I_v(t) \geq 0.$$

Thus, all state variables remain non-negative. □

2.5.2 Boundedness of solutions

Theorem 2.7 (Boundedness of solutions)**.** *The solutions of system* (24) *are bounded in the feasible region*

$$\Omega_e = \left\{ (S, I_e, R, S_v, I_v) \in \mathbb{R}^5_+ : N_c \leq \frac{\Lambda_c}{\mu_c},\ N_v \leq \frac{\Lambda_v}{\mu_v} \right\},$$

where $N_c = S + I_e + R$ *and* $N_v = S_v + I_v$.

Proof. For the total cattle population:

$$\frac{dN_c}{dt} = \Lambda_c - \mu_c N_c \implies N_c(t) \leq \frac{\Lambda_c}{\mu_c}.$$

For the total tick population:

$$\frac{dN_v}{dt} = \Lambda_v - \mu_v N_v \implies N_v(t) \leq \frac{\Lambda_v}{\mu_v}.$$

Hence, solutions remain bounded in Ω_e. □

2.5.3 Disease-free equilibrium (DFE)

The disease-free equilibrium of the ECF-only system is

$$\mathbf{E}_{e0} = \left(\frac{\Lambda_c}{\mu_c}, 0, 0, \frac{\Lambda_v}{\mu_v}, 0 \right). \tag{25}$$

2.5.4 Basic reproduction number

Let $\mathbf{x} = (I_e, I_v)^T$ denote the infected compartments. Using the next-generation matrix approach:

$$\mathcal{F} = \begin{pmatrix} \beta_e S I_v \\ \alpha_v S_v I_e \end{pmatrix}, \quad \mathcal{V} = \begin{pmatrix} (\gamma_e + \mu_c) I_e \\ \mu_v I_v \end{pmatrix}.$$

Evaluating at $\mathbf{E}_{e0}$ gives

$$F = \begin{pmatrix} 0 & \beta_e \frac{\Lambda_c}{\mu_c} \\ \alpha_v \frac{\Lambda_v}{\mu_v} & 0 \end{pmatrix}, \quad V = \begin{pmatrix} \gamma_e + \mu_c & 0 \\ 0 & \mu_v \end{pmatrix}.$$

The next-generation matrix is $K = FV^{-1}$, and the basic reproduction number is

$$\mathcal{R}_{e0} = \sqrt{\frac{\beta_e \alpha_v \Lambda_c \Lambda_v}{\mu_c (\gamma_e + \mu_c) \mu_v^2}}. \tag{26}$$

2.5.5 Local stability of the DFE

To investigate local stability, we first compute the Jacobian matrix of system (24) in terms of partial derivatives:

$$\mathcal{J}(S, I_e, R, S_v, I_v) = \begin{pmatrix} \frac{\partial \dot{S}}{\partial S} & \frac{\partial \dot{S}}{\partial I_e} & \frac{\partial \dot{S}}{\partial R} & \frac{\partial \dot{S}}{\partial S_v} & \frac{\partial \dot{S}}{\partial I_v} \\ \frac{\partial \dot{I}_e}{\partial S} & \frac{\partial \dot{I}_e}{\partial I_e} & \frac{\partial \dot{I}_e}{\partial R} & \frac{\partial \dot{I}_e}{\partial S_v} & \frac{\partial \dot{I}_e}{\partial I_v} \\ \frac{\partial \dot{R}}{\partial S} & \frac{\partial \dot{R}}{\partial I_e} & \frac{\partial \dot{R}}{\partial R} & \frac{\partial \dot{R}}{\partial S_v} & \frac{\partial \dot{R}}{\partial I_v} \\ \frac{\partial \dot{S}_v}{\partial S} & \frac{\partial \dot{S}_v}{\partial I_e} & \frac{\partial \dot{S}_v}{\partial R} & \frac{\partial \dot{S}_v}{\partial S_v} & \frac{\partial \dot{S}_v}{\partial I_v} \\ \frac{\partial \dot{I}_v}{\partial S} & \frac{\partial \dot{I}_v}{\partial I_e} & \frac{\partial \dot{I}_v}{\partial R} & \frac{\partial \dot{I}_v}{\partial S_v} & \frac{\partial \dot{I}_v}{\partial I_v} \end{pmatrix}. \tag{27}$$

From (24), the partial derivatives are:

$$\begin{array}{lllll} \frac{\partial \dot{S}}{\partial S} = -\beta_e I_v - \mu_c, & \frac{\partial \dot{S}}{\partial I_e} = 0, & \frac{\partial \dot{S}}{\partial R} = 0, & \frac{\partial \dot{S}}{\partial S_v} = 0, & \frac{\partial \dot{S}}{\partial I_v} = -\beta_e S, \\ \frac{\partial \dot{I}_e}{\partial S} = \beta_e I_v, & \frac{\partial \dot{I}_e}{\partial I_e} = -(\gamma_e + \mu_c), & \frac{\partial \dot{I}_e}{\partial R} = 0, & \frac{\partial \dot{I}_e}{\partial S_v} = 0, & \frac{\partial \dot{I}_e}{\partial I_v} = \beta_e S, \\ \frac{\partial \dot{R}}{\partial S} = 0, & \frac{\partial \dot{R}}{\partial I_e} = \gamma_e, & \frac{\partial \dot{R}}{\partial R} = -\mu_c, & \frac{\partial \dot{R}}{\partial S_v} = 0, & \frac{\partial \dot{R}}{\partial I_v} = 0, \\ \frac{\partial \dot{S}_v}{\partial S} = 0, & \frac{\partial \dot{S}_v}{\partial I_e} = -\alpha_v S_v, & \frac{\partial \dot{S}_v}{\partial R} = 0, & \frac{\partial \dot{S}_v}{\partial S_v} = -\alpha_v I_e - \mu_v, & \frac{\partial \dot{S}_v}{\partial I_v} = 0, \\ \frac{\partial \dot{I}_v}{\partial S} = 0, & \frac{\partial \dot{I}_v}{\partial I_e} = \alpha_v S_v, & \frac{\partial \dot{I}_v}{\partial R} = 0, & \frac{\partial \dot{I}_v}{\partial S_v} = \alpha_v I_e, & \frac{\partial \dot{I}_v}{\partial I_v} = -\mu_v. \end{array}$$

Evaluating (27) at the disease-free equilibrium $\mathbf{E}_{e0} = \left(\frac{\Lambda_c}{\mu_c}, 0, 0, \frac{\Lambda_v}{\mu_v}, 0\right)$ gives the Jacobian matrix:

$$\mathcal{J}_0 = \begin{pmatrix} -\mu_c & 0 & 0 & 0 & -\beta_e \frac{\Lambda_c}{\mu_c} \\ 0 & -(\gamma_e + \mu_c) & 0 & 0 & \beta_e \frac{\Lambda_c}{\mu_c} \\ 0 & \gamma_e & -\mu_c & 0 & 0 \\ 0 & -\alpha_v \frac{\Lambda_v}{\mu_v} & 0 & -\mu_v & 0 \\ 0 & \alpha_v \frac{\Lambda_v}{\mu_v} & 0 & 0 & -\mu_v \end{pmatrix}. \tag{28}$$

The eigenvalues of $\mathcal{J}_0$ can be determined by the characteristic equation, and we obtain:

$$\lambda_1 = -\mu_c, \quad \lambda_2 = -\mu_c, \quad \lambda_3 = -\mu_v.$$

$$\lambda_4 = -\frac{\mu_c\mu_v^2 + (\gamma_e\mu_c + \mu_c^2)\mu_v - \sqrt{4\,\Lambda_c\Lambda_v\alpha_v\beta_e\mu_c\mu_v + \mu_c^2\mu_v^4 - 2\,(\gamma_e\mu_c^2 + \mu_c^3)\mu_v^3 + (\gamma_e^2\mu_c^2 + 2\,\gamma_e\mu_c^3 + \mu_c^4)\mu_v^2}}{2\,\mu_c\mu_v},$$

$$\lambda_5 = -\frac{\mu_c\mu_v^2 + (\gamma_e\mu_c + \mu_c^2)\mu_v + \sqrt{4\,\Lambda_c\Lambda_v\alpha_v\beta_e\mu_c\mu_v + \mu_c^2\mu_v^4 - 2\,(\gamma_e\mu_c^2 + \mu_c^3)\mu_v^3 + (\gamma_e^2\mu_c^2 + 2\,\gamma_e\mu_c^3 + \mu_c^4)\mu_v^2}}{2\,\mu_c\mu_v}.$$

Looking at λ_4 we get:

$$\begin{aligned}
\lambda_4 &= -\frac{\mu_c\mu_v^2 + (\gamma_e\mu_c + \mu_c^2)\,\mu_v - \sqrt{4\,\Lambda_c\Lambda_v\alpha_v\beta_e\mu_c\mu_v + \mu_c^2\mu_v^4 - 2\,(\gamma_e\mu_c^2 + \mu_c^3)\,\mu_v^3 + (\gamma_e^2\mu_c^2 + 2\gamma_e\mu_c^3 + \mu_c^4)\,\mu_v^2}}{2\,\mu_c\mu_v} \\
&= -\frac{\mu_v}{2\mu_c}\,(\mu_v + \gamma_e + \mu_c) + \frac{1}{2\mu_c\mu_v}\sqrt{4\Lambda_c\Lambda_v\alpha_v\beta_e\mu_c\mu_v + \mu_c^2\mu_v^4 - 2(\gamma_e\mu_c^2 + \mu_c^3)\mu_v^3 + (\gamma_e^2\mu_c^2 + 2\gamma_e\mu_c^3 + \mu_c^4)\mu_v^2} \\
&= -\frac{\mu_v}{2\mu_c}\,(\mu_v + \gamma_e + \mu_c) + \sqrt{\frac{4\Lambda_c\Lambda_v\alpha_v\beta_e\mu_c\mu_v}{4\mu_c^2\mu_v^2} + \frac{\mu_c^2\mu_v^4 - 2(\gamma_e\mu_c^2 + \mu_c^3)\mu_v^3 + (\gamma_e^2\mu_c^2 + 2\gamma_e\mu_c^3 + \mu_c^4)\mu_v^2}{4\mu_c^2\mu_v^2}} \\
&= \mathcal{R}_{e01} + \sqrt{\mathcal{R}_{e02}^2 + \mathcal{R}_{e03}},
\end{aligned}$$

where

$$\begin{aligned}
\mathcal{R}_{e01} &= -\frac{\mu_v}{2\mu_c}\,(\mu_v + \gamma_e + \mu_c)\,, \\
\mathcal{R}_{e02} &= \sqrt{\frac{4\Lambda_c\Lambda_v\alpha_v\beta_e\mu_c\mu_v}{4\mu_c^2\mu_v^2}}, \\
\mathcal{R}_{e03} &= \frac{\mu_c^2\mu_v^4 - 2(\gamma_e\mu_c^2 + \mu_c^3)\mu_v^3 + (\gamma_e^2\mu_c^2 + 2\gamma_e\mu_c^3 + \mu_c^4)\mu_v^2}{4\mu_c^2\mu_v^2}.
\end{aligned}$$

In the same way for λ_5 we get

$$\begin{aligned}
\lambda_5 &= -\frac{\mu_c\mu_v^2 + (\gamma_e\mu_c + \mu_c^2)\,\mu_v + \sqrt{4\,\Lambda_c\Lambda_v\alpha_v\beta_e\mu_c\mu_v + \mu_c^2\mu_v^4 - 2\,(\gamma_e\mu_c^2 + \mu_c^3)\,\mu_v^3 + (\gamma_e^2\mu_c^2 + 2\,\gamma_e\mu_c^3 + \mu_c^4)\,\mu_v^2}}{2\,\mu_c\mu_v} \\
&= -\frac{\mu_v\,(\mu_c\mu_v + (\gamma_e\mu_c + \mu_c^2))}{2\mu_c\mu_v} - \frac{1}{2\mu_c\mu_v}\sqrt{4\Lambda_c\Lambda_v\alpha_v\beta_e\mu_c\mu_v + \mu_c^2\mu_v^4 - 2(\gamma_e\mu_c^2 + \mu_c^3)\mu_v^3 + (\gamma_e^2\mu_c^2 + 2\gamma_e\mu_c^3 + \mu_c^4)\mu} \\
&= -\frac{\mu_v}{2\mu_c}\,(\mu_v + \gamma_e + \mu_c) - \frac{1}{2\mu_c\mu_v}\sqrt{4\Lambda_c\Lambda_v\alpha_v\beta_e\mu_c\mu_v + \mu_c^2\mu_v^4 - 2(\gamma_e\mu_c^2 + \mu_c^3)\mu_v^3 + (\gamma_e^2\mu_c^2 + 2\gamma_e\mu_c^3 + \mu_c^4)\mu_v^2} \\
&= \mathcal{R}'_{e01} - \sqrt{{\mathcal{R}'_{e02}}^2 + \mathcal{R}'_{e03}},
\end{aligned}$$

where,

$$\begin{aligned}
\mathcal{R}'_{e01} &= -\frac{\mu_v}{2\mu_c}\,(\mu_v + \gamma_e + \mu_c)\,, \\
\mathcal{R}'_{e02} &= \sqrt{\frac{4\Lambda_c\Lambda_v\alpha_v\beta_e\mu_c\mu_v}{4\mu_c^2\mu_v^2}}, \\
\mathcal{R}'_{e03} &= \frac{\mu_c^2\mu_v^4 - 2(\gamma_e\mu_c^2 + \mu_c^3)\mu_v^3 + (\gamma_e^2\mu_c^2 + 2\gamma_e\mu_c^3 + \mu_c^4)\mu_v^2}{4\mu_c^2\mu_v^2}.
\end{aligned}$$

We now can observe the scenarios for λ_4 and λ_5 to be negative. It is clear that these conditions are:

- For λ_4 to be negative:

$$\mathcal{R}_{e02}^2 + \mathcal{R}_{e03} < \mathcal{R}_{e01}^2.$$

- For λ_5 to be negative:

$$\mathcal{R}'^2_{e02} + \mathcal{R}'_{e03} > |\mathcal{R}'_{e01}|$$

Thus, for both eigenvalues to be negative, we need:

$$\mathcal{R}^2_{e02} + \mathcal{R}_{e03} < \mathcal{R}^2_{e01} \quad \text{and} \quad \mathcal{R}'^2_{e02} + \mathcal{R}'_{e03} > |\mathcal{R}'_{e01}|$$

2.5.6 Endemic Equilibrium of the ECF-only Model

The endemic equilibrium corresponds to the persistent presence of ECF in both cattle and tick populations. To determine this equilibrium, we set

$$\dot{S} = \dot{I}_e = \dot{R} = \dot{S}_v = \dot{I}_v = 0.$$

This yields the system

$$\begin{aligned} \Lambda_c - \beta_e S I_v - \mu_c S &= 0, \\ \beta_e S I_v - (\gamma_e + \mu_c) I_e &= 0, \\ \gamma_e I_e - \mu_c R &= 0, \\ \Lambda_v - \alpha_v S_v I_e - \mu_v S_v &= 0, \\ \alpha_v S_v I_e - \mu_v I_v &= 0. \end{aligned} \tag{29}$$

From the third equation of (29), we obtain

$$R^* = \frac{\gamma_e}{\mu_c} I_e^*. \tag{30}$$

From the fifth equation,

$$I_v^* = \frac{\alpha_v S_v^* I_e^*}{\mu_v}. \tag{31}$$

Substituting this into the second equation of (29) gives

$$\beta_e S^* \left(\frac{\alpha_v S_v^* I_e^*}{\mu_v} \right) = (\gamma_e + \mu_c) I_e^*.$$

For $I_e^* > 0$, dividing by I_e^* yields

$$\beta_e \alpha_v S^* S_v^* = \mu_v (\gamma_e + \mu_c). \tag{32}$$

From the fourth equation of (29),

$$S_v^* = \frac{\Lambda_v}{\alpha_v I_e^* + \mu_v}. \tag{33}$$

Substituting this into (32), we obtain

$$\beta_e \alpha_v S^* \frac{\Lambda_v}{\alpha_v I_e^* + \mu_v} = \mu_v (\gamma_e + \mu_c).$$

Using the first equation of (29),

$$S^* = \frac{\Lambda_c}{\beta_e I_v^* + \mu_c}.$$

After substituting for I_v^* and simplifying, we obtain a nonlinear equation in I_e^* whose unique positive solution exists if and only if $\mathcal{R}_{e0} > 1$,

where

$$\mathcal{R}_{e0} = \sqrt{\frac{\beta_e \alpha_v \Lambda_c \Lambda_v}{\mu_c(\gamma_e + \mu_c)\mu_v^2}}. \tag{34}$$

Thus, whenever $\mathcal{R}_{e0} > 1$, there exists a unique positive solution I_e^*, and consequently

$$\mathbf{E}_e^* = \left(S^*,\ I_e^*,\ \frac{\gamma_e}{\mu_c} I_e^*,\ \frac{\Lambda_v}{\alpha_v I_e^* + \mu_v},\ \frac{\alpha_v S_v^* I_e^*}{\mu_v} \right). \tag{35}$$

Hence, the endemic equilibrium exists uniquely whenever $\mathcal{R}_{e0} > 1$.

Proposition 2.8 (Global Stability of the Endemic Equilibrium)**.** *If $\mathcal{R}_{e0} > 1$, the endemic equilibrium $\mathbf{E}_e^*$ of the ECF-only model is globally asymptotically stable in the interior of the feasible region Ω.*

Proof. Consider the ECF-only system

$$\dot{S} = \Lambda_c - \beta_e S I_v - \mu_c S, \tag{36}$$
$$\dot{I}_e = \beta_e S I_v - (\gamma_e + \mu_c) I_e, \tag{37}$$
$$\dot{R} = \gamma_e I_e - \mu_c R, \tag{38}$$
$$\dot{S}_v = \Lambda_v - \alpha_v S_v I_e - \mu_v S_v, \tag{39}$$
$$\dot{I}_v = \alpha_v S_v I_e - \mu_v I_v. \tag{40}$$

From the total population dynamics

$$\dot{N}_c = \dot{S} + \dot{I}_e + \dot{R} = \Lambda_c - \mu_c N_c, \qquad \dot{N}_v = \dot{S}_v + \dot{I}_v = \Lambda_v - \mu_v N_v,$$

it follows that

$$N_c(t) \to \frac{\Lambda_c}{\mu_c}, \qquad N_v(t) \to \frac{\Lambda_v}{\mu_v} \quad \text{as } t \to \infty.$$

Hence the dynamics reduce asymptotically to the infected subsystem (I_e, I_v), with

$$S = \frac{\Lambda_c}{\mu_c} - I_e - R \approx \frac{\Lambda_c}{\mu_c} - \left(1 + \frac{\gamma_e}{\mu_c}\right) I_e, \tag{41}$$
$$S_v = \frac{\Lambda_v}{\mu_v} - I_v. \tag{42}$$

Substituting (41) and (42) into (37) and (40), the planar infected subsystem becomes

$$\begin{aligned} \dot{I}_e &= \beta_e \left(\frac{\Lambda_c}{\mu_c} - \left(1 + \frac{\gamma_e}{\mu_c}\right) I_e \right) I_v - (\gamma_e + \mu_c) I_e, \\ \dot{I}_v &= \alpha_v \left(\frac{\Lambda_v}{\mu_v} - I_v \right) I_e - \mu_v I_v. \end{aligned} \tag{43}$$

Let the Dulac function $B(I_e, I_v) = \frac{1}{I_e I_v}$. Then

$$\begin{aligned} \frac{\partial}{\partial I_e}(B\dot{I}_e) + \frac{\partial}{\partial I_v}(B\dot{I}_v) &= \frac{\partial}{\partial I_e}\left(\frac{\dot{I}_e}{I_e I_v}\right) + \frac{\partial}{\partial I_v}\left(\frac{\dot{I}_v}{I_e I_v}\right) \\ &= -\frac{\beta_e \left(\frac{\Lambda_c}{\mu_c} - \left(1 + \frac{\gamma_e}{\mu_c}\right) I_e\right)}{I_e^2} - \frac{\alpha_v \left(\frac{\Lambda_v}{\mu_v} - I_v\right)}{I_v^2} \\ &< 0 \quad \text{for all } (I_e, I_v) \in \mathbb{R}^2_+. \end{aligned}$$

By the Bendixson–Dulac criterion, the planar system (43) admits no periodic orbits in the interior of the feasible region.

When $\mathcal{R}_{e0} > 1$, the disease-free equilibrium is unstable, and solutions in the interior remain bounded away from the boundary, implying uniform persistence. By the Poincaré–Bendixson theorem, any bounded trajectory of the planar system converges to an equilibrium point. Since the endemic equilibrium (I_e^*, I_v^*) is unique and lies in the interior, all interior trajectories converge to (I_e^*, I_v^*).

Finally, the remaining variables S, R, and S_v are uniquely determined by (I_e^*, I_v^*). Therefore, the full endemic equilibrium

$$\mathbf{E}_e^* = (S^*, I_e^*, R^*, S_v^*, I_v^*)$$

is globally asymptotically stable in the interior of the feasible region Ω whenever $\mathcal{R}_{e0} > 1$. □

2.6 Qualitative Analysis of the FMD–ECF Co-infection Model

In this section, we analyze the qualitative properties of the model describing the co-infection dynamics of Foot-and-Mouth Disease (FMD) and East Coast Fever (ECF) in cattle. The analysis focuses on the existence of equilibrium points, the basic reproduction numbers, and the stability of the disease-free equilibrium (DFE). Our approach relies on the next generation matrix framework of van den Driessche & Watmough (2002) and standard techniques from host–vector epidemiology.

The cattle population is subdivided into susceptible, singly infected, co-infected, and recovered classes, while the tick population is subdivided into susceptible and infected classes. Transmission of ECF occurs via vector-borne interactions, whereas FMD spreads through direct cattle-to-cattle contact.

We consider the system of ordinary differential equations (1) describing the co-infection

dynamics of Foot-and-Mouth Disease (FMD) and East Coast Fever (ECF):

$$\begin{aligned}
\dot{S} &= \Lambda_c - \beta_e S I_v - \beta_f S I_f - \mu_c S,\\
\dot{I}_e &= \beta_e S I_v - (\eta_{ef} + \gamma_e + \mu_c) I_e,\\
\dot{I}_f &= \beta_f S I_f - (\eta_{fe} + \gamma_f + \mu_c) I_f,\\
\dot{I}_{ef} &= \eta_{ef} I_e + \eta_{fe} I_f - (\gamma_{ef} + \mu_c) I_{ef},\\
\dot{R} &= \gamma_e I_e + \gamma_f I_f + \gamma_{ef} I_{ef} - \mu_c R,\\
\dot{S}_v &= \Lambda_v - \alpha_v S_v (I_e + I_{ef}) - \mu_v S_v,\\
\dot{I}_v &= \alpha_v S_v (I_e + I_{ef}) - \mu_v I_v.
\end{aligned} \tag{44}$$

2.6.1 Model Feasibility and Boundedness

The total cattle and vector populations satisfy:

$$N_c = S + I_e + I_f + I_{ef} + R, \quad N_v = S_v + I_v.$$

From (44) we obtain

$$\dot{N}_c = \Lambda_c - \mu_c N_c \implies \lim_{t\to\infty} N_c(t) = \frac{\Lambda_c}{\mu_c}, \quad \dot{N}_v = \Lambda_v - \mu_v N_v \implies \lim_{t\to\infty} N_v(t) = \frac{\Lambda_v}{\mu_v}. \tag{45}$$

Define the feasible region

$$\Gamma = \left\{ (S, I_e, I_f, I_{ef}, R, S_v, I_v) \in \mathbb{R}^7_+ : N_c \le \frac{\Lambda_c}{\mu_c}, N_v \le \frac{\Lambda_v}{\mu_v} \right\}. \tag{46}$$

Remark 2.9. *Using standard comparison theorems,* Γ *is positively invariant under the flow of* (44)*. Thus, solutions starting in* Γ *remain in* Γ *for all* $t \ge 0$*.*

2.6.2 Local Stability of the DFE

Using the next generation matrix (as in the previous sections), it can be shown that the DFE $\mathbf{E}_0$ is locally asymptotically stable if $\mathcal{R}_0 < 1$, and unstable if $\mathcal{R}_0 > 1$. Furthermore, the system exhibits a transcritical bifurcation at $\mathcal{R}_0 = 1$, which marks the threshold between disease extinction and persistence, with satisfactory details in Theorem 2.10 for a particular case. This implies that small increases in the reproduction number above unity can lead to the emergence of an endemic state.

Theorem 2.10. *The system* (1) *undergoes a forward (supercritical) transcritical bifurcation at* $\mathcal{R}_{0,e} = 1$ *with respect to the bifurcation parameter* β_e*.*

Proof. Let β_e be the bifurcation parameter and denote $\varepsilon = \mathcal{R}_{0,e} - 1$. At $\mathcal{R}_{0,e} = 1$, the disease–free equilibrium

$$P_0 = \left(\frac{\Lambda_c}{\mu_c}, 0, 0, 0, 0, \frac{\Lambda_v}{\mu_v}, 0 \right)$$

has a simple zero eigenvalue, while all other eigenvalues have negative real parts.

Let $X = (I_e, I_v)$ denote the variables corresponding to the critical two–dimensional subsystem (ECF host–vector cycle). After translation of the equilibrium and suitable linear transformation, the system can be written in the form

$$\begin{cases} \dot{y} = \lambda z + F_1(y, z), \\ \dot{z} = F_2(y, z), \end{cases}$$

where $\lambda = 0$ at $\mathcal{R}_{0,e} = 1$ and $F_1, F_2 = O(\|(y, z)\|^2)$.

Assume the center manifold has the form

$$y = h(z) = u_{20}z^2 + u_{30}z^3 + O(z^4).$$

Differentiating with respect to time,

$$\frac{dy}{dt} = 2u_{20}z\frac{dz}{dt} + 3u_{30}z^2\frac{dz}{dt} + O(\|(y, z)\|^4).$$

Substituting into the system and comparing coefficients of like powers of z, we obtain the determining equations for the coefficients. Solving them yields

$$u_{20} = -\frac{\beta_e S^0}{A_e}, \qquad u_{30} = \frac{\beta_e^2 (S^0)^2}{A_e^2},$$

where $A_e = \eta_{ef} + \gamma_e + \mu_c$.

Substituting $y = h(z)$ into the z–equation gives

$$\frac{dz}{dt} = a_{20}z^2 + a_{30}z^3 + O(z^4),$$

where

$$a_{20} = \frac{\beta_e \alpha_v S^0 S_v^0}{\mu_v} - A_e, \qquad a_{30} = -\frac{\beta_e^2 \alpha_v (S^0)^2 S_v^0}{\mu_v A_e}.$$

At the bifurcation point $\mathcal{R}_{0,e} = 1$, we have

$$\beta_e \alpha_v S^0 S_v^0 = A_e \mu_v,$$

so that the quadratic coefficient changes sign with ε.

Hence near $\mathcal{R}_{0,e} = 1$,

$$\frac{dz}{dt} = \varepsilon z - cz^2 + O(z^3),$$

where

$$c = \frac{\beta_e^2 \alpha_v (S^0)^2 S_v^0}{\mu_v A_e} > 0.$$

Let

$$x_1 = z, \qquad x_2 = \dot{z}.$$

After successive coordinate transformations eliminating higher–order non–resonant terms, the system reduces to

$$\begin{cases} \dot{x}_1 = x_2, \\ \dot{x}_2 = \varepsilon x_1 - c x_1^2 + O(\|x\|^3). \end{cases}$$

Performing a time rescaling and near–identity transformation yields the canonical normal form

$$\dot{u} = \varepsilon u - c u^2 + O(u^3).$$

Since $c > 0$, the equilibrium $u = 0$ exchanges stability with the non–trivial equilibrium $u = \varepsilon/c$ as ε passes through zero.

Therefore, the system undergoes a forward (supercritical) transcritical bifurcation at $\mathcal{R}_{0,e} = 1$. □

Remark 2.11. *The co-infection transition parameters η_{ef} and η_{fe} represent the rate at which singly infected cattle acquire the second infection. Although these parameters do not affect the invasion thresholds $\mathcal{R}_{f0}$ and $\mathcal{R}_{e0}$, they directly influence the endemic levels of co-infected cattle (I_{ef}) and the distribution of infection among host compartments.*

2.7 Global Stability Analysis of the FMD–ECF Co-infection Model

To perform a rigorous and detailed global stability analysis for the co-infection model, we utilize the matrix-theoretic method for the disease-free equilibrium (DFE) (Shuai & Van Den Driessche, 2013)a and Volterra-type Lyapunov functions for the endemic equilibrium (EE) (Guo & Li, 2006; Bentaleb *et al.*, 2019).

2.7.1 Disease-Free Equilibrium (DFE)

The disease-free equilibrium (DFE) is

$$P_0 = (S^0, 0, 0, 0, 0, S_v^0, 0) = \left(\frac{\Lambda_c}{\mu_c}, 0, 0, 0, 0, \frac{\Lambda_v}{\mu_v}, 0 \right). \tag{47}$$

Using the next generation matrix method, let the infected vector be

$$x = (I_e, I_f, I_{ef}, I_v)^T,$$

and decompose the system as

$$\dot{x} = F(x) - V(x),$$

where $F(x)$ denotes new infection terms and $V(x)$ other transitions.

At the DFE, the Jacobians are

$$F = \begin{pmatrix} 0 & 0 & 0 & \beta_e S^0 \\ 0 & \beta_f S^0 & 0 & 0 \\ 0 & 0 & 0 & 0 \\ \alpha_v S_v^0 & 0 & \alpha_v S_v^0 & 0 \end{pmatrix}, \quad V = \begin{pmatrix} k_e & 0 & 0 & 0 \\ 0 & k_f & 0 & 0 \\ -\eta_{ef} & -\eta_{fe} & k_{ef} & 0 \\ 0 & 0 & 0 & \mu_v \end{pmatrix}, \tag{48}$$

where

$$k_e = \eta_{ef} + \gamma_e + \mu_c, \quad k_f = \eta_{fe} + \gamma_f + \mu_c, \quad k_{ef} = \gamma_{ef} + \mu_c.$$

The next generation matrix is $K = FV^{-1}$ and the basic reproduction number is

$$R_0 = \rho(FV^{-1}) = \max\{R_{f0}, R_{e0}\}, \tag{49}$$

with

$$R_{f0} = \frac{\beta_f S^0}{k_f} = \frac{\beta_f \Lambda_c}{\mu_c(\eta_{fe} + \gamma_f + \mu_c)}, \quad R_{e0} = \sqrt{\frac{\beta_e \alpha_v S^0 S_v^0}{\mu_v k_e}} = \sqrt{\frac{\beta_e \alpha_v \Lambda_c \Lambda_v}{\mu_c \mu_v^2 (\eta_{ef} + \gamma_e + \mu_c)}}.$$

2.7.2 Global Stability of the DFE

Theorem 2.12 (Global Stability of DFE)**.** *If $\mathcal{R}_0 \leq 1$, the disease-free equilibrium P_0 is globally asymptotically stable (GAS) in Γ.*

Proof. Let q^T be the left Perron eigenvector of $V^{-1}F$ such that $q^T V^{-1} F = \mathcal{R}_0 q^T$. Define for model (1) the Lyapunov function

$$Q = q^T V^{-1} x.$$

Differentiating along trajectories of (44):

$$\dot{Q} = q^T V^{-1} \dot{x} = q^T V^{-1}(F(x) - V(x))x \leq (\mathcal{R}_0 - 1)\, q^T x.$$

Since $S \leq S^0$ and $S_v \leq S_v^0$ in Γ, we have $F(x)x \leq Fx$. Hence, if $\mathcal{R}_0 \leq 1$, $\dot{Q} \leq 0$ with equality only at P_0. By LaSalle's Invariance Principle (see (Haddad & Chellaboina, 2008)), P_0 is GAS in Γ. □

2.7.3 Global Stability of the Endemic Equilibrium

Theorem 2.13 (Global Stability of EE)**.** *If $\mathcal{R}_0 > 1$, the endemic equilibrium $P^* = (S^*, I_e^*, I_f^*, I_{ef}^*, R^*, S_v^*, I_v^*)$ is globally asymptotically stable in int(Γ).*

Proof. Let a Volterra-type Lyapunov function:

$$V = \left(S - S^* - S^* \ln \frac{S}{S^*}\right) + c_1 \left(I_e - I_e^* - I_e^* \ln \frac{I_e}{I_e^*}\right) + c_2 \left(I_f - I_f^* - I_f^* \ln \frac{I_f}{I_f^*}\right)$$
$$+ c_3 \left(S_v - S_v^* - S_v^* \ln \frac{S_v}{S_v^*}\right) + c_4 \left(I_v - I_v^* - I_v^* \ln \frac{I_v}{I_v^*}\right),$$

with positive constants c_i to be determined.

Differentiating V along the trajectories and using equilibrium relations (e.g., $\Lambda_c = \beta_e S^* I_v^* + \beta_f S^* I_f^* + \mu_c S^*$) yields

$$\dot{V} \leq 0,$$

where each grouped term is non-positive by the Arithmetic-Geometric Mean inequality:

$$\sqrt{a_1 a_2 \dots a_n} \leq \frac{a_1 + a_2 + \cdots + a_n}{n}$$

It follows that the equality $\dot{V} = 0$ holds only at P^* (Al Agha *et al.*,2022). Therefore, by the Lyapunov–LaSalle theorem (see (LaSalle, 1987)), the endemic equilibrium is globally asymptotically stable in $int(\Gamma)$. □

Remark 2.14. *The co-infection parameters η_{ef} and η_{fe}, while not affecting the invasion threshold R_0, directly determine the equilibrium levels of co-infected cattle I^*_{ef}, influencing the distribution of infection across host compartments.*

2.8 Sensitivity Analysis

In this section, we perform a sensitivity analysis to assess the influence of model parameters on the basic reproduction number $\mathcal{R}_0$. Sensitivity analysis provides insight into which epidemiological and demographic parameters most strongly affect disease transmission and therefore represent effective targets for intervention strategies.

The normalized forward sensitivity index of $\mathcal{R}_0$ with respect to a parameter P is defined as (Abdulrahman *et al.*, 2013)

$$L_P^{\mathcal{R}_0} = \frac{\partial \mathcal{R}_0}{\partial P} \cdot \frac{P}{\mathcal{R}_0}. \tag{50}$$

This index measures the relative change in $\mathcal{R}_0$ induced by a relative change in the parameter P.

Recall that the basic reproduction number of the co-infection system is given by

$$\mathcal{R}_0 = \max\left\{\mathcal{R}_{f0}, \mathcal{R}_{e0}\right\},$$

where $\mathcal{R}_{f0}$ and $\mathcal{R}_{e0}$ denote the basic reproduction numbers associated with Foot-and-Mouth Disease (FMD) and East Coast Fever (ECF), respectively. Consequently, the sensitivity indices of $\mathcal{R}_0$ are evaluated through the dominant sub-reproduction number.

The FMD reproduction number is given by

$$\mathcal{R}_{f0} = \frac{\beta_f S^*}{\eta_{fe} + \gamma_f + \mu_c} = \frac{\beta_f \Lambda_c}{\mu_c\left(\eta_{fe} + \gamma_f + \mu_c\right)}, \tag{51}$$

while the ECF reproduction number is

$$\mathcal{R}_{e0} = \sqrt{\frac{\beta_e \alpha_v S^* S_v^*}{\mu_v\left(\eta_{ef} + \gamma_e + \mu_c\right)}} = \sqrt{\frac{\beta_e \alpha_v \Lambda_c \Lambda_v}{\mu_c \mu_v^2\left(\eta_{ef} + \gamma_e + \mu_c\right)}}. \tag{52}$$

2.8.1 Illustrative Sensitivity Analysis for $\mathcal{R}_{f0}$

To illustrate the computation of sensitivity indices, we consider the FMD reproduction number $\mathcal{R}_{f0}$ defined in (51). We compute sensitivity indices with respect to the FMD transmission rate β_f and the cattle recruitment rate Λ_c.

Sensitivity with respect to β_f Differentiating $\mathcal{R}_{f0}$ with respect to β_f yields

$$\frac{\partial \mathcal{R}_{f0}}{\partial \beta_f} = \frac{\Lambda_c}{\mu_c\left(\eta_{fe} + \gamma_f + \mu_c\right)}.$$

Substituting into (50), we obtain

$$L_{\beta_f}^{\mathcal{R}_0} = \frac{\Lambda_c}{\mu_c\left(\eta_{fe} + \gamma_f + \mu_c\right)} \cdot \frac{\beta_f}{\mathcal{R}_{f0}} = 1.$$

Hence, a 1% increase in the FMD transmission rate leads to a 1% increase in $\mathcal{R}_{f0}$.

Sensitivity with respect to Λ_c Similarly, differentiating $\mathcal{R}_{f0}$ with respect to Λ_c gives

$$\frac{\partial \mathcal{R}_{f0}}{\partial \Lambda_c} = \frac{\beta_f}{\mu_c\left(\eta_{fe} + \gamma_f + \mu_c\right)}.$$

The corresponding sensitivity index is

$$L_{\Lambda_c}^{\mathcal{R}_0} = \frac{\beta_f}{\mu_c\left(\eta_{fe} + \gamma_f + \mu_c\right)} \cdot \frac{\Lambda_c}{\mathcal{R}_{f0}} = 1.$$

Thus, $\mathcal{R}_{f0}$ is linearly sensitive to changes in the cattle recruitment rate.

2.8.2 Illustrative Sensitivity Analysis for $\mathcal{R}_{e0}$

We now consider the ECF reproduction number $\mathcal{R}_{e0}$ given in (52). We focus on the sensitivity indices with respect to the transmission rate β_e and the vector transmission rate α_v.

Sensitivity with respect to β_e Differentiating $\mathcal{R}_{e0}$ with respect to β_e yields

$$\frac{\partial \mathcal{R}_{e0}}{\partial \beta_e} = \frac{1}{2}\sqrt{\frac{\alpha_v \Lambda_c \Lambda_v}{\mu_c \mu_v^2 (\eta_{ef} + \gamma_e + \mu_c)\beta_e}} = \frac{1}{2}\frac{\mathcal{R}_{e0}}{\beta_e}.$$

The normalized forward sensitivity index is then

$$L_{\beta_e}^{\mathcal{R}_0} = \frac{\partial \mathcal{R}_{e0}}{\partial \beta_e} \cdot \frac{\beta_e}{\mathcal{R}_{e0}} = \frac{1}{2}. \tag{53}$$

Sensitivity with respect to α_v Similarly, differentiating $\mathcal{R}_{e0}$ with respect to α_v gives

$$\frac{\partial \mathcal{R}_{e0}}{\partial \alpha_v} = \frac{1}{2}\frac{\mathcal{R}_{e0}}{\alpha_v}.$$

Thus, the corresponding sensitivity index is

$$L_{\alpha_v}^{\mathcal{R}_0} = \frac{\partial \mathcal{R}_{e0}}{\partial \alpha_v} \cdot \frac{\alpha_v}{\mathcal{R}_{e0}} = \frac{1}{2}. \tag{54}$$

Hence, a 1% increase in either the host-to-vector transmission rate β_e or the vector infection rate α_v results in a 0.5% increase in $\mathcal{R}_{e0}$, indicating moderate sensitivity of ECF spread to these parameters.

Sensitivity with respect to μ_v We note that in (52) μ_v appears squared in the denominator under the square root, so more precisely:

$$\mathcal{R}_{e0} = \sqrt{\frac{\beta_e \alpha_v \Lambda_c \Lambda_v}{\mu_c \mu_v^2 (\eta_{ef} + \gamma_e + \mu_c)}} \quad \Rightarrow \quad \frac{\partial \mathcal{R}_{e0}}{\partial \mu_v} = -\frac{\mathcal{R}_{e0}}{\mu_v}.$$

The normalized forward sensitivity index is then

$$L_{\mu_v}^{\mathcal{R}_0} = \frac{\partial \mathcal{R}_{e0}}{\partial \mu_v} \cdot \frac{\mu_v}{\mathcal{R}_{e0}} = -1. \tag{55}$$

We see that a 1% increase in the tick mortality rate μ_v leads to a 1% decrease in $\mathcal{R}_{e0}$, showing that $\mathcal{R}_{e0}$ is highly sensitive to changes in tick survival.

Remark 2.15. *From (52), it is evident that the ECF reproduction number $\mathcal{R}_{e0}$ is strongly influenced by the tick-to-cattle transmission rate β_e, the cattle-to-tick transmission rate α_v, and the tick mortality rate μ_v. In particular, $\mathcal{R}_{e0}$ exhibits negative sensitivity with respect to μ_v, highlighting the importance of vector control strategies. A complete numerical sensitivity analysis of all parameters, based on the values listed in Table 4, is presented in Table 3.*

Parameter	**Sensitivity ($\mathcal{R}_{f0}$)**	**Sensitivity ($\mathcal{R}_{e0}$)**
Λ_c	1.0000	0.5000
Λ_v	0.0000	0.5000
μ_c	−1.0079	−0.5076
μ_v	0.0000	−0.9999
β_e	0.0000	0.5000
β_f	1.0000	0.0000
α_v	0.0000	0.5000
γ_e	0.0000	−0.1894
γ_f	−0.7936	0.0000
η_{ef}	0.0000	−0.3030
η_{fe}	−0.1984	0.0000

Table 3: Normalized forward sensitivity indices of $\mathcal{R}_{f0}$ (FMD) and $\mathcal{R}_{e0}$ (ECF) with respect to key model parameters.

3 Optimal Control Analysis

We aim to minimize the objective function $\mathbb{O}(u)$ in (56), which incorporates both the infection burden in the cattle population and the costs associated with intervention strategies. The objective function is given by:

$$\mathbb{O}(u) = \int_0^T \left(c_1 I_e + c_2 I_f + c_3 I_{ef} + c_4 R + c_5 S_v + d_1 \frac{u_1^2}{2} + d_2 \frac{u_2^2}{2} + d_3 \frac{u_3^2}{2} \right) dt \tag{56}$$

where:

- c_1, c_2, c_3, c_4, c_5 are positive weights that represent the relative importance of reducing the infection burden in the susceptible (S_c), infected (I_e, I_f, and I_{ef}), and vector (S_v) populations,
- d_1, d_2, d_3 are positive weights for the costs associated with the control variables u_1, u_2, and u_3, which represent vaccination, treatment, and vector control, respectively.

The model dynamics, which include the evolution of cattle populations, infected and co-infected compartments, and the effects of intervention strategies, are governed by the following system (57) of differential equations:

$$\begin{aligned}
\min[\mathbb{O}(u)] &= \int_0^T \left(c_1 I_e + c_2 I_f + c_3 I_{ef} + c_4 R + c_5 S_v + d_1 \frac{u_1^2}{2} + d_2 \frac{u_2^2}{2} + d_3 \frac{u_3^2}{2} \right) dt, \\
\dot{S} &= \Lambda_c - (1-u_3)\beta_e S I_v - (1-u_3)\beta_f S I_f - \mu_c S - u_1 S, \\
\dot{I}_e &= (1-u_3)\beta_e S I_v - (\eta_{ef} + \gamma_e + \mu_c) I_e - u_2 I_e, \\
\dot{I}_f &= (1-u_3)\beta_f S I_f - (\eta_{fe} + \gamma_f + \mu_c) I_f - u_2 I_f, \\
\dot{I_{ef}} &= \eta_{ef} I_e + \eta_{fe} I_f - (\gamma_{ef} + \mu_c) I_{ef} - u_2 I_{ef}, \\
\dot{R} &= \gamma_e I_e + \gamma_f I_f + \gamma_{ef} I_{ef} - \mu_c R + u_1 S, \\
\dot{S}_v &= \Lambda_v - (1-u_3)\alpha_v S_v (I_e + I_{ef}) - \mu_v S_v, \\
\dot{I}_v &= (1-u_3)\alpha_v S_v (I_e + I_{ef}) - \mu_v I_v, \\
S(0) &= S_0, \quad I_e(0) = I_{e0}, \quad I_f(0) = I_{f0}, \quad I_{ef}(0) = I_{ef0}, \quad R(0) = R_0, \\
S_v(0) &= S_{v0}, \quad I_v(0) = I_{v0}.
\end{aligned} \tag{57}$$

Here, $u_1(t), u_2(t), u_3(t)$ represent the time-dependent control variables associated with vaccination, treatment, and vector control strategies, respectively.

To find the optimal control, we apply Pontryagin's Maximum Principle (PMP) (Pontryagin, 1987). The Hamiltonian H is given by:

$$H = c_1 I_e + c_2 I_f + c_3 I_{ef} + c_4 R + c_5 S_v + d_1 \frac{u_1^2}{2} + d_2 \frac{u_2^2}{2} + d_3 \frac{u_3^2}{2} + p_S \dot{S} + p_{I_e} \dot{I}_e + p_{I_f} \dot{I}_f + p_{I_{ef}} \dot{I_{ef}} + p_R \dot{R} + p_{S_v} \dot{S}_v + p_{I_v} \dot{I}_v.$$

Here, $p = (p_S, p_{I_e}, p_{I_f}, p_{I_{ef}}, p_R, p_{S_v}, p_{I_v})$ is the adjoint vector. To find the optimal control $u^* = (u_1^*(t), u_2^*(t), u_3^*(t))$, we solve the following conditions:

$$\frac{\partial H}{\partial u_i} = 0, \quad i = 1, 2, 3$$

and the adjoint system is governed by:

$$\dot{p}_i = -\frac{\partial H}{\partial x_i}, \quad i = 1, \ldots, 7, \quad p_i(T) = 0, \quad i = 1, \ldots, 7.$$

The optimal control laws are given by:

$$u_1^*(t) = \min\left(u_1^{\max}, \max\left(0, \frac{(p_R - p_S)S}{d_1}\right)\right),$$
$$u_2^*(t) = \min\left(u_2^{\max}, \max\left(0, \frac{p_{I_e}I_e + p_{I_f}I_f + p_{I_{ef}}I_{ef}}{d_2}\right)\right),$$
$$u_3^*(t) = \min\left(u_3^{\max}, \max\left(0, \frac{(p_{I_e} - p_S)\beta_e SI_v + (p_{I_f} - p_S)\beta_f SI_f + (p_{I_{ef}} - p_S)(\eta_{ef}I_e + \eta_{fe}I_f)}{d_3}\right)\right).$$

Let $(S^*, I_e^*, I_f^*, I_{ef}^*, R^*, S_v^*, I_v^*)$ be the optimal state variables solution associated with the optimal control variable u^* subject to the control problem. Then, there exists an adjoint vector $p = (p_S, p_{I_e}, p_{I_f}, p_{I_{ef}}, p_R, p_{S_v}, p_{I_v})$ that satisfies the controlled system, with transversality conditions $p_i(T) = 0$ for $i = 1, \ldots, 7$, where the optimal controls are:

$$u_1^*(t) = \frac{(p_R - p_S)S}{d_1},$$
$$u_2^* = \frac{p_{I_e}I_e + p_{I_f}I_f + p_{I_{ef}}I_{ef}}{d_2},$$
$$u_3^*(t) = \frac{(p_{I_e} - p_S)\beta_e SI_v + (p_{I_f} - p_S)\beta_f SI_f + (p_{I_{ef}} - p_S)(\eta_{ef}I_e + \eta_{fe}I_f)}{d_3}.$$

To observe this, we start with the Hamiltonian system. Using PMP, we derive the adjoint equations for the state variables, and we show that the optimal controls can be expressed in terms of the adjoint variables. The Hamiltonian H is given by:

$$H = c_1I_e + c_2I_f + c_3I_{ef} + c_4R + c_5S_v + d_1\frac{u_1^2}{2} + d_2\frac{u_2^2}{2} + d_3\frac{u_3^2}{2} + p_S\dot{S} + p_{I_e}\dot{I}_e + p_{I_f}\dot{I}_f + p_{I_{ef}}\dot{I}_{ef} + p_R\dot{R} + p_{S_v}\dot{S}_v + p_{I_v}\dot{I}_v.$$

Here, $p = (p_S, p_{I_e}, p_{I_f}, p_{I_{ef}}, p_R, p_{S_v}, p_{I_v})$ is the adjoint vector.
The adjoint system is as follows:

$$\begin{aligned}
\frac{dp_S}{dt} &= -\frac{\partial H}{\partial S} = p_S\left[(1-u_3)\beta_e I_v + (1-u_3)\beta_f I_f + \mu_c + u_1\right] - p_{I_e}(1-u_3)\beta_e I_v \\
&\quad - p_{I_f}(1-u_3)\beta_f I_f - p_{I_{ef}}(1-u_3)\eta_{ef} I_e \\
&\quad - p_R\gamma_e I_e - p_{S_v}\alpha_v S_v(I_e + I_{ef}), \\
\frac{dp_{I_e}}{dt} &= -\frac{\partial H}{\partial I_e} = p_{I_e}\left[(1-u_3)\beta_e S I_v - (\eta_{ef} + \gamma_e + \mu_c)\right] + p_{I_{ef}}\eta_{ef}, \\
\frac{dp_{I_f}}{dt} &= -\frac{\partial H}{\partial I_f} = p_{I_f}\left[(1-u_3)\beta_f S I_f - (\eta_{fe} + \gamma_f + \mu_c)\right] + p_{I_{ef}}\eta_{fe}, \\
\frac{dp_{I_{ef}}}{dt} &= -\frac{\partial H}{\partial I_{ef}} = p_{I_{ef}}(\gamma_{ef} + \mu_c) + p_{I_e}\eta_{ef} + p_{I_f}\eta_{fe}, \\
\frac{dp_R}{dt} &= -\frac{\partial H}{\partial R} = -p_R(\mu_c), \\
\frac{dp_{S_v}}{dt} &= -\frac{\partial H}{\partial S_v} = p_{S_v}\left[(1-u_3)\alpha_v(I_e + I_{ef}) - \mu_v\right], \\
\frac{dp_{I_v}}{dt} &= -\frac{\partial H}{\partial I_v} = p_{I_v}\left[(1-u_3)\alpha_v S_v(I_e + I_{ef}) - \mu_v\right].
\end{aligned}$$

Now, according to PMP, the optimal control laws are derived from the following conditions:

$$\frac{\partial H}{\partial u_1} = d_1 u_1 - (p_R - p_S)\, S = 0,$$

$$\frac{\partial H}{\partial u_2} = d_2 u_2 - (p_{I_e} I_e + p_{I_f} I_f + p_{I_{ef}} I_{ef}) = 0,$$

$$\frac{\partial H}{\partial u_3} = d_3 u_3 - \left[(p_{I_e} - p_S)\beta_e S I_v + (p_{I_f} - p_S)\beta_f S I_f + (p_{I_{ef}} - p_S)(\eta_{ef} I_e + \eta_{fe} I_f)\right] = 0.$$

Solving these optimality conditions, we obtain the following optimal control laws:

$$\begin{aligned}
u_1^*(t) &= \min\left(u_1^{\max}, \max\left(0, \frac{(p_R - p_S)S}{d_1}\right)\right), \\
u_2^*(t) &= \min\left(u_2^{\max}, \max\left(0, \frac{p_{I_e} I_e + p_{I_f} I_f + p_{I_{ef}} I_{ef}}{d_2}\right)\right), \\
u_3^*(t) &= \min\left(u_3^{\max}, \max\left(0, \frac{(p_{I_e} - p_S)\beta_e S I_v + (p_{I_f} - p_S)\beta_f S I_f + (p_{I_{ef}} - p_S)(\eta_{ef} I_e + \eta_{fe} I_f)}{d_3}\right)\right).
\end{aligned}$$

Thus, the optimal control laws are determined.

4 Results and Discussion

In this section, we present numerical simulations of the ECF–FMD co-infection model (1) to explore the dynamics of disease spread in cattle and the impact of optimal intervention strategies. Parameter values used in the simulations are summarized in Table 4, with assumed values for illustrative purposes.

We investigate the effects of vaccination of susceptible cattle, treatment of infected cattle, and tick/vector control on the dynamics of single and co-infected cattle populations. The optimal control problem (57) is solved numerically to determine time-dependent strategies that minimize infection prevalence while balancing the costs of interventions. These simulations provide insights into the effectiveness and timing of combined control measures, highlighting the importance of managing co-infections to reduce the overall disease burden in cattle populations.

Parameter	**Value**	**Units**	**Source**
Λ_c	2	heads/day	Assumed
Λ_v	80	ticks/day	Assumed
μ_c	0.002	day^{-1}	Assumed
μ_v	0.10	day^{-1}	Assumed
β_e	0.30	day^{-1}	Assumed
β_f	0.10	day^{-1}	Assumed
α_v	0.35	day^{-1}	Assumed
γ_e	0.05	day^{-1}	Assumed
γ_f	0.20	day^{-1}	Assumed
γ_{ef}	0.03	day^{-1}	Assumed
η_{ef}	0.08	day^{-1}	Assumed
η_{fe}	0.05	day^{-1}	Assumed

Table 4: Model parameters, their values, and sources used in the numerical implementation.

To quantify the influence of model parameters on the basic reproduction numbers, we computed the normalized forward sensitivity indices of $\mathcal{R}_f$ (FMD) and $\mathcal{R}_e$ (ECF) with respect to each parameter in the model. Figure 2 presents horizontal bar charts of these indices for all relevant parameters.

As shown in Table 3, the normalized forward sensitivity indices reveal the relative influence of each model parameter on the basic reproduction numbers $\mathcal{R}_{f0}$ (FMD) and $\mathcal{R}_{e0}$ (ECF). For FMD, we observe that the cattle recruitment rate Λ_c and the FMD transmission rate β_f have the strongest positive effect on $\mathcal{R}_{f0}$, with sensitivity indices of 1.0000 (see Figure 2). This indicates that a 1% increase in either Λ_c or β_f would result in approximately a 1% increase in $\mathcal{R}_{f0}$. In contrast, the cattle natural death rate μ_c and the FMD recovery rate γ_f have strong negative effects, reducing $\mathcal{R}_{f0}$ when increased. The co-infection rate η_{fe} also contributes negatively, but to a lesser extent. On the other hand, for ECF, the most influential parameters are the tick natural death rate μ_v, the cattle recruitment rate Λ_c, the tick recruitment rate Λ_v, and the transmission rates β_e and α_v, each with sensitivity indices

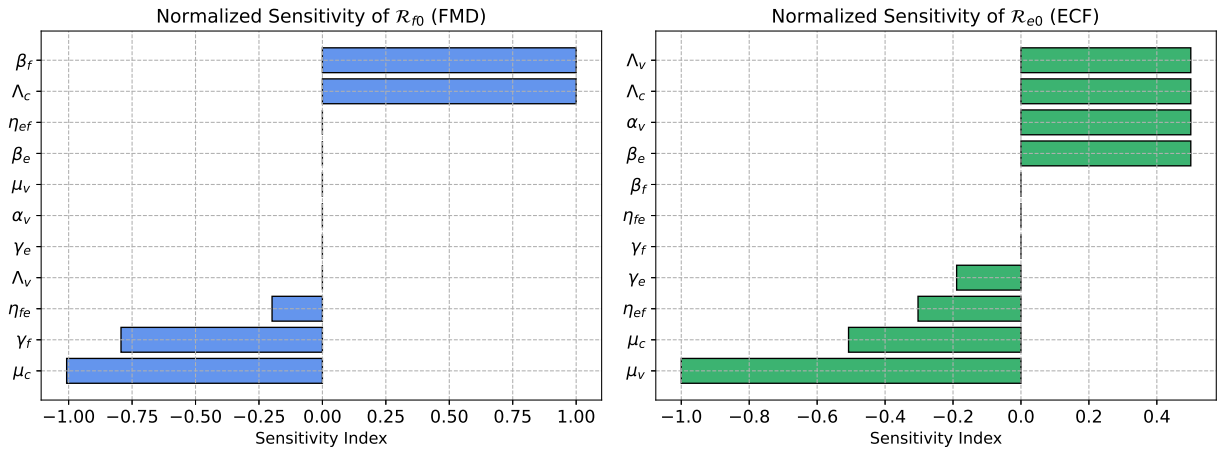

Figure 2: Normalized sensitivity indices of (left) $\mathcal{R}_f$ (FMD) and (right) $\mathcal{R}_e$ (ECF). Positive values indicate that an increase in the parameter increases the reproduction number, whereas negative values indicate an inverse effect.

around 0.5 or -1.0. This reflects the vector-borne nature of ECF, where both tick and cattle dynamics strongly affect disease transmission. Recovery from ECF (γ_e) and the rate at which ECF-infected cattle acquire FMD (η_{ef}) reduce $\mathcal{R}_{e0}$ moderately, as indicated by their negative sensitivity indices. Overall, the sensitivity analysis highlights which epidemiological and demographic parameters are most critical for disease control. For FMD, interventions targeting cattle recruitment or transmission could substantially reduce $\mathcal{R}_{f0}$, while for ECF, controlling tick populations or reducing vector-to-host transmission would have the greatest impact on $\mathcal{R}_{e0}$.

Remark 4.1. *Since the basic reproduction number of the co-infection system is defined as*

$$\mathcal{R}_0 = \max\left\{\mathcal{R}_{f0}, \mathcal{R}_{e0}\right\},$$

the overall epidemic potential is determined by the pathogen with the larger reproduction number. Based on the baseline parameter values from Table 4, we have $\mathcal{R}_{f0} \approx 396.8254$ *and* $\mathcal{R}_{e0} \approx 2522.6249$. *Therefore, ECF dominates the system dynamics. And, this is the main case in the African community including Malawi as evident from the studies of Muthiru & Bukachi (2025), Oligo* et al.*, (2023), and Muthiru* et al.*, (2025).*

As can be seen in Table 3, the parameters contributing most to $\mathcal{R}_{f0}$ *are the cattle recruitment rate* $\Lambda_c = 2.0$ *heads/day and the FMD transmission rate* $\beta_f = 0.10$ *day*$^{-1}$, *both with a sensitivity index of 1.0000. The cattle natural death rate* $\mu_c = 0.002$ *day*$^{-1}$ *and the FMD recovery rate* $\gamma_f = 0.20$ *day*$^{-1}$ *exert strong negative effects on* $\mathcal{R}_{f0}$, *while the co-infection rate* $\eta_{fe} = 0.05$ *day*$^{-1}$ *has a moderate negative influence. This indicates that interventions aimed at reducing cattle-to-cattle transmission (e.g., vaccination or reducing contact rates) and controlling cattle recruitment can have the most substantial impact on lowering the overall reproduction number* $\mathcal{R}_0$, *as FMD is currently the dominant driver of the epidemic.*

The simulation results shown in Figure 3 illustrate the behavior of the ECF-FMD co-infection system when the populations are initialized near the disease-free equilibrium (DFE).

As expected from the high basic reproduction numbers ($\mathcal{R}_{f0} \approx 396.83$ for FMD and $\mathcal{R}_{e0} \approx 2522.62$ for ECF), the DFE is unstable. Small introductions of infection quickly lead to increases in the infected compartments (I_e, I_f, I_{ef}) and the infectious tick population (I_v), while the susceptible populations (S and S_v) decrease correspondingly.

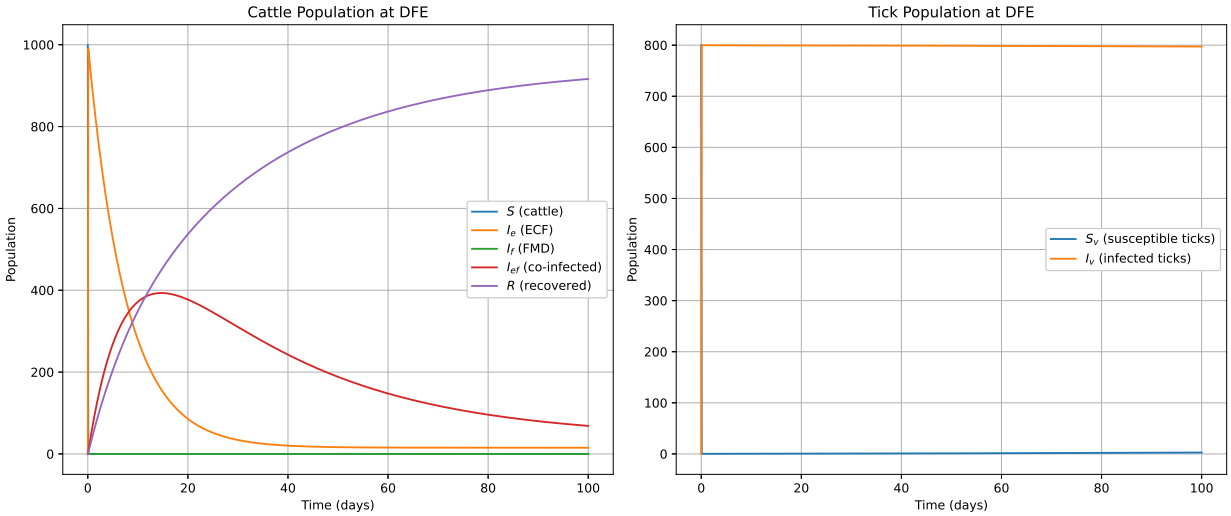

Figure 3: Dynamics of cattle and tick populations near the DFE. The left panel shows the cattle compartments: susceptible (S), ECF-infected (I_e), FMD-infected (I_f), and co-infected (I_{ef}). The right panel shows the tick compartments: susceptible ticks (S_v) and ECF-infectious ticks (I_v).

This behavior indicates that, under the given parameter values, both FMD and ECF have a strong potential to establish and maintain endemicity in the cattle population. In particular, the extremely high $\mathcal{R}_{e0}$ suggests that ECF spreads rapidly among both cattle and ticks, driving the tick infection dynamics and amplifying the co-infection risk. These findings are consistent with field observations in Malawi, where ECF is reported to be highly endemic in smallholder and commercial cattle system. Foot-and-Mouth Disease also exhibits recurrent outbreaks, often co-occurring with other infections, reflecting the significant influence of cattle-to-cattle transmission (high β_f) and cattle recruitment rates (Λ_c) on the system dynamics. Thus, interventions targeting reduction of transmission (e.g., vaccination, tick control) are critical to prevent establishment of endemic states.

Having noticed that the DFE was unstable, with infected populations persisting over time, we implemented targeted modifications to key epidemiological parameters to reduce the basic reproduction numbers $\mathcal{R}_{f0}$ and $\mathcal{R}_{e0}$ below unity. These modifications were subject to the findings in Table 3. By decreasing cattle-to-cattle transmission β_f, vector-to-cattle transmission β_e, and co-infection rates η_{ef} and η_{fe}, while slightly increasing recovery rates γ_f and γ_e, we ensured that both $\mathcal{R}_{f0} < 1$ and $\mathcal{R}_{e0} < 1$.

This adjustment stabilizes the DFE, as can be seen in Figure 4, where the infected compartments I_e, I_f, I_{ef}, and I_v gradually decay to zero over time, while susceptible populations S and S_v stabilize at their equilibrium values $S^* = \Lambda_c/\mu_c$ and $S_v^* = \Lambda_v/\mu_v$. The dynamics confirm that under these targeted parameter modifications, disease transmission cannot sustain itself, and both FMD and ECF die out in the long term.

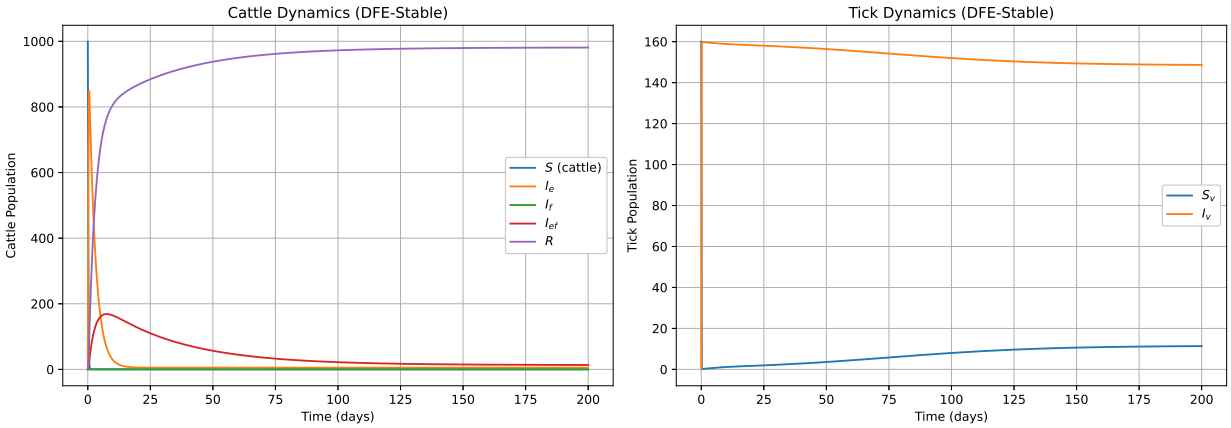

Figure 4: Simulation of the ECF-FMD co-infection model at the stabilized DFE. In this simulation, the parameters were adjusted to reduce the reproduction numbers below 1: $\mathcal{R}_{f0} = 0.8510$, $\mathcal{R}_{e0} = 0.5134$, $\beta_f = 0.005$, $\beta_e = 0.05$, $\gamma_f = 0.5$, $\gamma_e = 0.3$, $\mu_c = 0.002$, $\mu_v = 0.5$, $\Lambda_c = 2$, $\Lambda_v = 80$, $\alpha_v = 0.35$. The susceptible populations S (cattle) and S_v (ticks) remain near their DFE values, while the infected populations decay to zero, illustrating a stable disease-free state.

Having observed that the Disease-Free Equilibrium (DFE) was unstable under the baseline parameters, we allowed the system to evolve over time from a small initial infection. As expected from the theoretical analysis, the infected compartments did not decay to zero but instead approached positive steady-state values, indicating the presence of an endemic equilibrium. This transition from the unstable DFE to the endemic state is illustrated in Figure 5.

To simulate the optimal control problem, we employed the estimated weight parameters for both the infection burden and the control costs as summarized in Table 5. These weights, denoted by c_1, c_2, c_3, c_4 for the state variables and d_1, d_2, d_3 for the control variables, were chosen to reflect the relative importance of reducing infection levels and the costs associated with vaccination, treatment, and vector control.

Parameter	**Value**	**Description / Units**
c_1	0.5	Weight for ECF-infected cattle (I_e)
c_2	0.5	Weight for FMD-infected cattle (I_f)
c_3	0.5	Weight for co-infected cattle (I_{ef})
c_4	0.5	Weight for recovered cattle (R)
d_1	10^4	Cost weight for vaccination control (u_1)
d_2	10^6	Cost weight for treatment control (u_2)
d_3	5×10^5	Cost weight for vector control (u_3)

Table 5: Weights used in the optimal control objective function for the ECF-FMD co-infection model.

To investigate the effects of control strategies on the dynamics of ECF-FMD co-infection

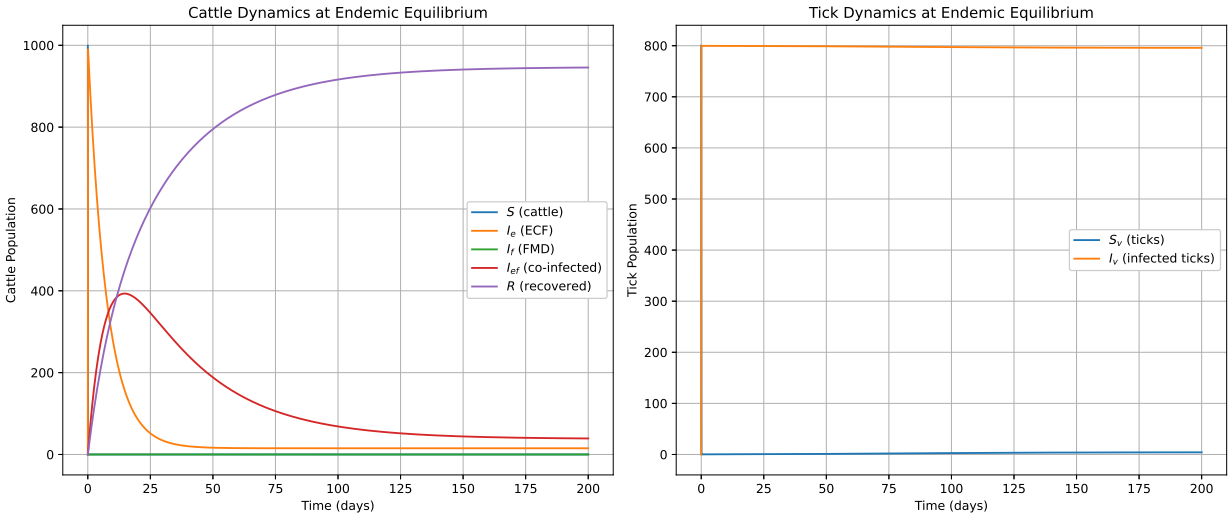

Figure 5: Simulation of the ECF–FMD co-infection model showing the system approaching the endemic equilibrium. The baseline parameters used are: $\Lambda_c = 2$, $\Lambda_v = 80$, $\mu_c = 0.002$, $\mu_v = 0.10$, $\beta_e = 0.30$, $\beta_f = 0.10$, $\alpha_v = 0.35$, $\gamma_e = 0.05$, $\gamma_f = 0.20$, $\gamma_{ef} = 0.03$, $\eta_{ef} = 0.08$, $\eta_{fe} = 0.05$. The corresponding reproduction numbers are $\mathcal{R}_{f0} = 396.8254$, $\mathcal{R}_{e0} = 2522.6249$, and $\mathcal{R}_0 = \max\{\mathcal{R}_{f0}, \mathcal{R}_{e0}\} = 2522.6249$.

in cattle and ticks, we numerically simulated the model over a period of 100 days under two scenarios: *with control* and *no control*. The control measures considered include vaccination, treatment, and vector-targeted interventions. The results are illustrated in Figure 6.

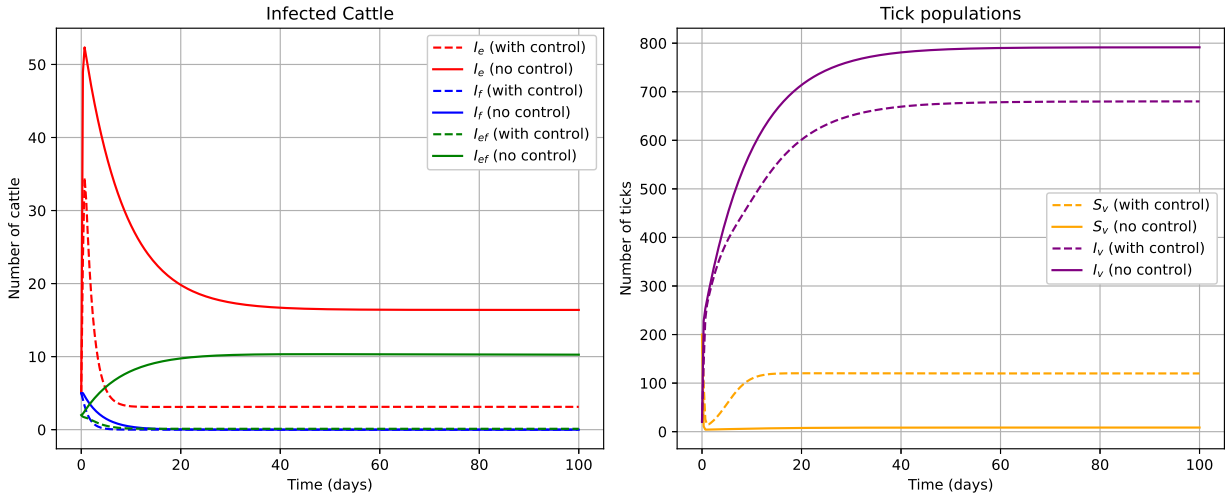

Figure 6: Dynamics of infected cattle (I_e, I_f, I_{ef}) and tick populations (S_v, I_v) with and without control measures over 100 days. Controlled scenarios are shown with dashed lines.

As shown in Figure 6, the implementation of control measures markedly alters the infection dynamics. In the absence of interventions, the number of infected cattle initially decreases but stabilizes at a steady level, indicating the persistence of infection within the

population. By contrast, when vaccination, treatment, and vector control are applied, the number of infected cattle declines rapidly to near zero within the first 20 days. This demonstrates the effectiveness of control measures in preventing widespread infection and promoting a disease-free state in the cattle population.

The tick population exhibits a similar response. Without control, the total tick population increases and reaches a high equilibrium, with a substantial fraction being infected, sustaining the risk of disease transmission. In the controlled scenario, the total tick population is limited, and the number of infected ticks is significantly reduced. Moreover, the susceptible tick population stabilizes at a higher level under control measures, reflecting the interruption of transmission dynamics. Overall, both cattle and tick populations reach a steady state after approximately 40 days, with the controlled system approaching a disease-free equilibrium for cattle and a lower equilibrium for ticks.

These results underscore the importance of integrated control strategies. By simultaneously targeting vaccination, treatment, and vector populations, the spread of co-infections can be effectively mitigated, reducing both infection prevalence and associated livestock mortality. The numerical simulations highlight that well-timed and appropriately scaled interventions are crucial for achieving stable disease-free conditions in livestock systems.

As illustrated in Figure 7, the response surface shows the combined effect of vaccination (u_1) and treatment (u_2) on the number of co-infected cattle (I_{ef}). The horizontal axes represent the control levels, ranging from 0.0 to 1.0, while the vertical axis corresponds to the co-infected population. The color gradient indicates the magnitude of I_{ef}.

The surface visibly bends downward as either control increases, forming a concave shape. This bending downward indicates that increasing vaccination or treatment reduces the number of co-infected cattle. The effect is synergistic: the lowest point on the surface (dark-blue color, near zero on the vertical axis) occurs when both u_1 and u_2 are close to 1. Conversely, when both controls are minimal, the surface rises to its highest values, indicating the largest number of co-infected cattle. Thus, the visualization in Figure 7 clearly demonstrates the effectiveness of combining vaccination and treatment strategies to control co-infection in the cattle population.

Again, Figure 8 depicts the impact of vaccination (u_1) and vector control (u_3) on the co-infected cattle population (I_{ef}). The horizontal axes correspond to the levels of the two interventions, while the vertical axis represents I_{ef}. The color scale reinforces the magnitude of the co-infected population, with darker shades indicating higher values.

The response surface demonstrates a pronounced downward curvature, bending toward the plane as both controls increase. This illustrates that enhancing either vaccination or vector control reduces the co-infected population. When both strategies are applied at high intensity, the surface reaches its minimum, indicating near-elimination of co-infection. In contrast, low levels of both controls correspond to elevated I_{ef} values. Overall, the figure highlights the combined efficacy of vaccination and vector-targeted interventions in mitigating co-infection.

Finally, Figure 9 illustrates how treatment (u_2) and vector control (u_3) jointly influence the co-infected cattle population (I_{ef}). The horizontal axes denote the control intensities, while the vertical axis indicates the number of co-infected cattle. The color gradient visually reinforces the vertical axis values, with deeper colors representing higher populations.

The surface exhibits a clear downward slope toward higher control levels, forming a con-

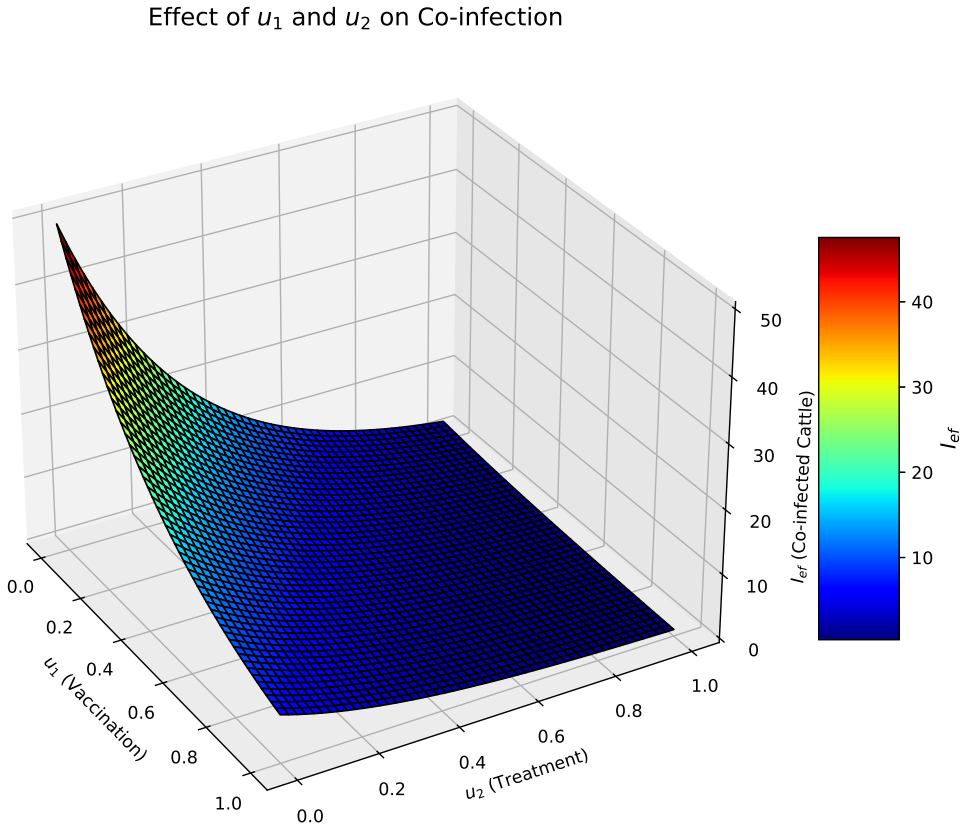

Figure 7: Co-infected cattle population I_{ef} as a function of vaccination u_1 and treatment u_2.

cave profile. This bending shows that increasing either treatment or vector control effectively lowers I_{ef}. The lowest values occur when both u_2 and u_3 are near their maximum, reflecting the strongest reduction in co-infection. Conversely, minimal controls correspond to the peak of the surface, with the highest co-infected population. The plot underscores the importance of simultaneously applying treatment and vector control to achieve optimal mitigation of co-infection in cattle.

As we can see in Figure 10, the implementation of control strategies significantly reduces the population of infected ticks. Increasing the levels of vaccination (u_1), treatment (u_2), and vector control (u_3) leads to a clear decline in the number of infected ticks across all pairwise combinations of controls. This reduction in the vector population directly contributes to a decrease in co-infection among cattle, highlighting the importance of combined intervention strategies in mitigating the spread of both FMD and ECF.

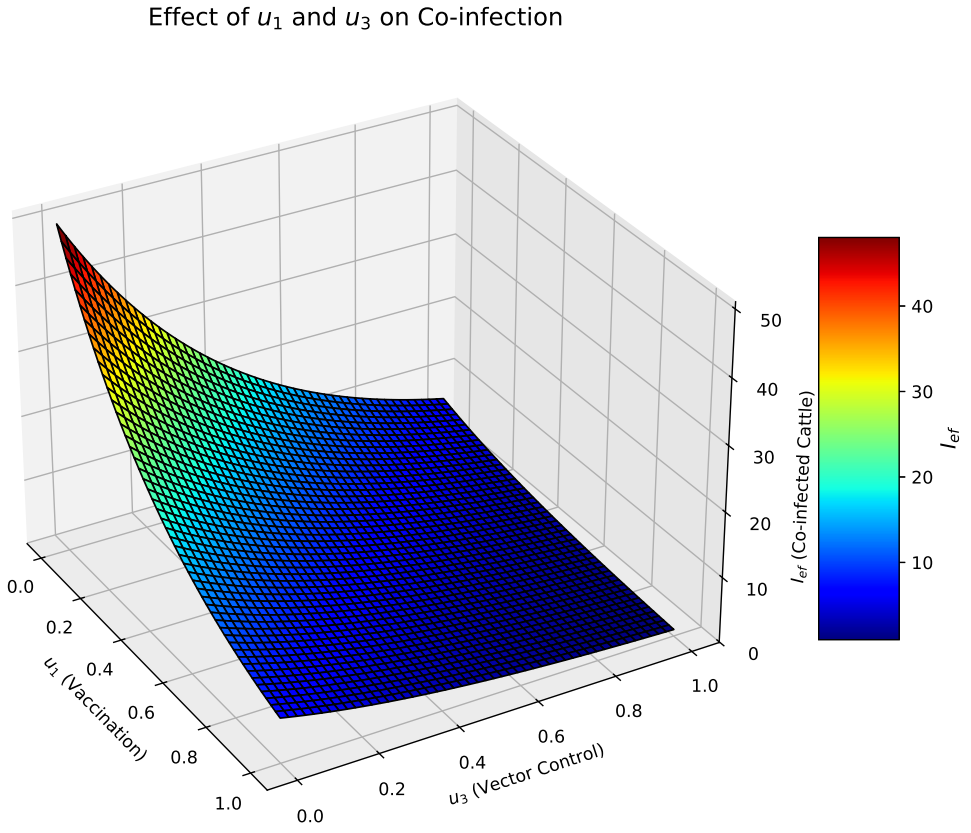

Figure 8: Co-infected cattle population I_{ef} as a function of vaccination u_1 and vector control u_3.

5 Conclusion

The persistent circulation of East Coast Fever (ECF) and Foot-and-Mouth Disease (FMD) in Malawi poses a major challenge to cattle production, particularly within smallholder and mixed farming systems where vector exposure, animal movement, and limited access to veterinary services facilitate disease transmission. The coexistence of these two infections creates favorable conditions for co-infection, with potential consequences for cattle health, productivity, and household livelihoods. Understanding the interaction between ECF and FMD is therefore essential for designing effective and sustainable disease control strategies.

In this study, a mathematical framework was developed to describe the transmission dynamics of ECF and FMD in a co-infected cattle population. The model incorporated direct cattle-to-cattle transmission for FMD and tick-mediated transmission for ECF, allowing for progression from single infection to co-infection. Qualitative analysis of the sub-models and the full system demonstrated that the disease-free equilibrium is unstable under baseline conditions, reflecting the endemic nature of ECF and the recurrent outbreaks of FMD observed in Malawi. Sensitivity analysis revealed that ECF dynamics are strongly driven by tick survival and vector-to-cattle transmission, while FMD transmission is primarily influenced by cattle recruitment and direct contact rates. These findings highlight the distinct

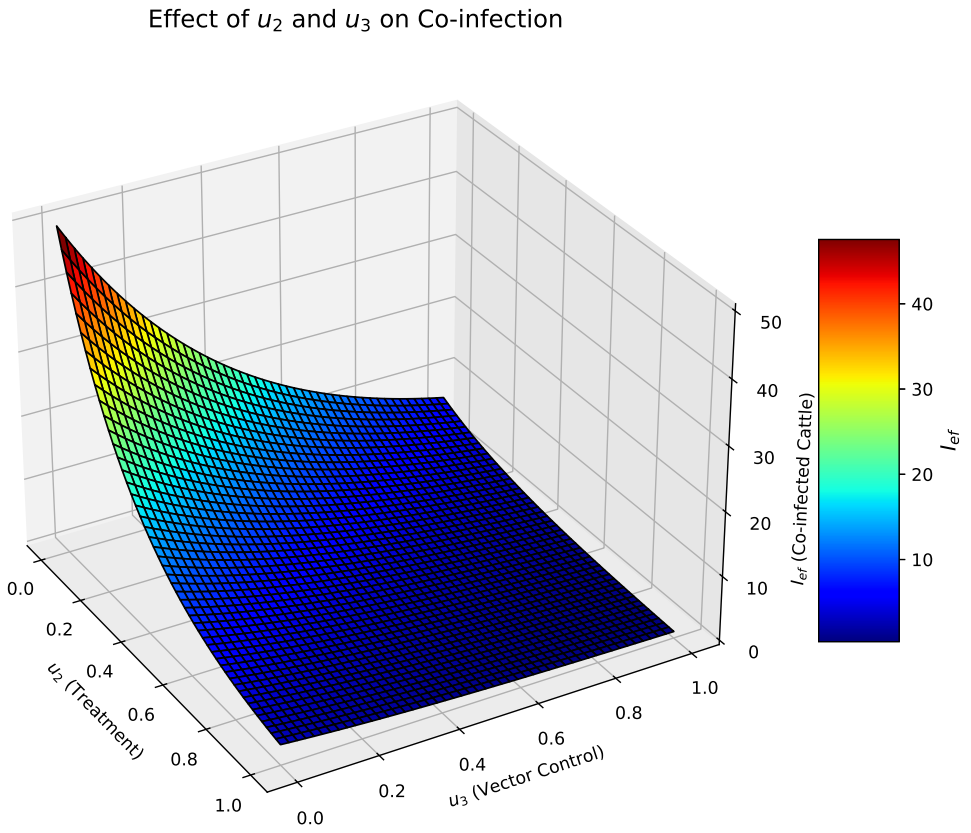

Figure 9: Co-infected cattle population I_{ef} as a function of treatment u_2 and vector control u_3.

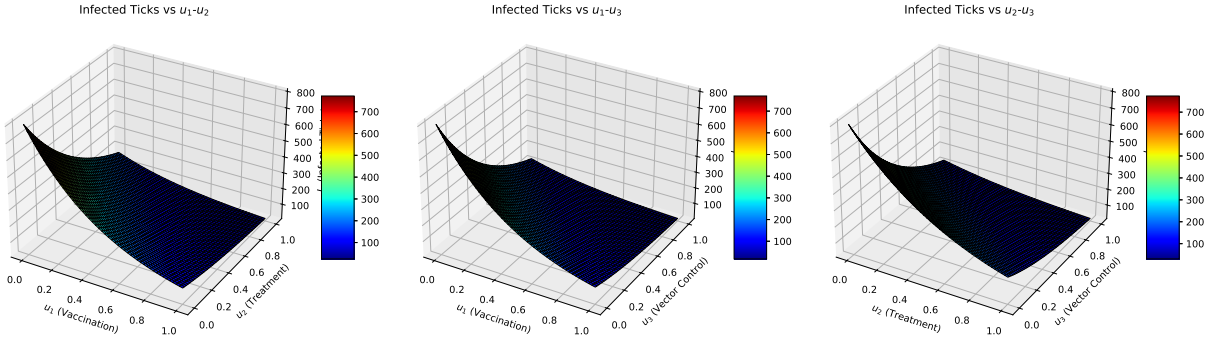

Figure 10: Effects of pairwise control strategies on the infected tick population. Left: u_1-u_2; Middle: u_1-u_3; Right: u_2-u_3.

but interacting mechanisms governing the spread of the two diseases.

Numerical simulations under different hypothetical scenarios, designed to reflect Malawian cattle production ecosystems, provided insight into the impact of co-infection and intervention strategies. The results showed that increases in transmission and co-infection rates lead to higher levels of co-infected cattle and sustained endemicity. In contrast, reducing

transmission parameters and enhancing recovery rates can stabilize the disease-free equilibrium. Furthermore, the optimal control analysis demonstrated that integrated intervention strategies of combining vaccination, treatment, and vector control are substantially more effective than single interventions in reducing infection prevalence and driving the system toward disease elimination. The findings of this study have important implications for livestock disease management in Malawi. In particular, they emphasize the critical role of vector control in managing ECF, alongside vaccination and treatment programs targeting FMD. The results support the implementation of coordinated, multi-pronged control strategies that simultaneously address cattle and tick populations, rather than focusing on individual diseases in isolation. Such integrated approaches have the potential to improve cattle productivity, reduce economic losses, and strengthen the resilience of smallholder farming systems.

Despite these contributions, the study has some limitations. The model was parameterized using assumed values and hypothetical scenarios due to the limited availability of detailed epidemiological data on ECF–FMD co-infection in Malawi. Consequently, the numerical results should be interpreted qualitatively rather than as precise quantitative predictions. In addition, the model does not explicitly account for spatial heterogeneity, seasonal variations in tick abundance, cattle movement patterns, or differences between production systems, all of which may influence disease dynamics in practice.

Future work should focus on incorporating field and surveillance data to improve parameter estimation and validate model predictions. Extensions of the model could include spatial structure, seasonal forcing, age-structured cattle populations, and explicit economic costs associated with disease and control measures. Moreover, incorporating stochastic effects and farmer behavior could provide a more realistic representation of disease dynamics under resource-limited settings. Overall, this study provides a foundational modelling framework for understanding ECF–FMD co-infection and offers a basis for future data-driven analyses to inform evidence-based livestock disease control policies in Malawi and similar settings.

Declarations

Clinical trial number: Not applicable.

Ethics approval and consent to participate: Not applicable. The study did not involve human participants, clinical trials, or animals requiring ethics approval.

Consent for publication: The authors hereby give consent for the publication of their details in the International Journal of Development Mathematics (IJDM).

Funding: The research received no funding.

Data Availability Statement: The data used in this study are derived from published literature and from numerical simulations of the mathematical model. No new experimental or observational data were generated. All parameter hypothesized values used in the

simulations are provided in the manuscript.

References

Banda, L. J., & Tanganyika, J. (2021). Livestock provide more than food in smallholder production systems of developing countries. *Animal Frontiers*, *11*(2), 7–14. https://doi.org/10.1093/af/vfab001

Herrero, M., Thornton, P. K., Gerber, P., & Reid, R. S. (2009). Livestock, livelihoods and the environment: understanding the trade-offs. *Current Opinion in Environmental Sustainability*, *1*(2), 111–120. https://doi.org/10.1016/j.cosust.2009.10.003

Herrero, M., Grace, D., Njuki, J., Johnson, N., Enahoro, D., Silvestri, S., & Rufino, M. C. (2013). The roles of livestock in developing countries. *Animal*, *7*, 3–18. https://doi.org/10.1017/S1751731112001954

Chatanga, E., et al. (2022). Tick-borne protozoan and rickettsial pathogens in cattle in Malawi. *Acta Tropica*, *231*, 106413. https://doi.org/10.1016/j.actatropica.2022.106413

Sibanda, B. (2014). Beef cattle development initiatives in Zimbabwe. *Global Journal of Animal Scientific Research*.

Minjauw, B., & McLeod, A. (2003). *Tick-borne diseases and poverty*. DFID Animal Health Programme, Edinburgh.

Monakale, K. S., et al. (2024). Ticks and tick-borne pathogens in South Africa. *Current Research in Parasitology & Vector-Borne Diseases*, *6*, 100205.

Djiman, T. A., Biguezoton, A. S., & Saegerman, C. (2024). Tick-borne diseases in Sub-Saharan Africa. *Pathogens*, *13*(8), 697.

Keeling, M. (2005). Models of foot-and-mouth disease. *Proceedings of the Royal Society B*, *272*, 1195–1202. https://doi.org/10.1098/rspb.2004.3046

Mumba, C., Skjerve, E., Rich, M., & Rich, K. M. (2017). Application of system dynamics in animal health. *PLOS ONE*, *12*(12), e0189878.

Wongnak, P., et al. (2024). A stochastic model of foot-and-mouth disease spread. *Preventive Veterinary Medicine*, *230*, 106282.

Shikumwifa, E. (2022). *Mathematical modeling of foot and mouth disease*. Master's thesis, University of Namibia.

Inayaturohmat, F., et al. (2024). Systematic review of coinfection models. *Journal of Multidisciplinary Healthcare*, *17*, 1091–1109.

Gilioli, G., Groppi, M., Vesperoni, M. P., Baumgärtner, J., & Gutierrez, A. P. (2009). An epidemiological model of East Coast fever in African livestock. *Ecological Modelling*, *220*(13), 1652–1662. https://doi.org/10.1016/j.ecolmodel.2009.03.017

Fahcruddin, I., Harianto, J., & Fitrial, D. (2023). Mathematical modeling of foot and mouth disease. *JTAM*.

Pesciaroli, M., et al. (2025). Modelling foot and mouth disease spread in livestock. *Animals*, *15*(3), 386.

Yano, T. K., Afrifa-Yamoah, E., Collins, J., Mueller, U., & Richardson, S. (2024). Mathematical modelling for co-infection diseases: A systematic review protocol. *BMJ Open*, *14*(12), e084027.

Hethcote, H. W. (2000). The mathematics of infectious diseases. *SIAM Review*, *42*(4), 599–653.

van den Driessche, P., & Watmough, J. (2002). Reproduction numbers and sub-threshold endemic equilibria. *Mathematical Biosciences*, *180*, 29–48.

Thieme, H. R. (2003). *Mathematics in Population Biology*. Princeton University Press.

Perko, L. (2001). *Differential Equations and Dynamical Systems* (3rd ed.). Springer-Verlag, New York.

Shuai, Z., & Van Den Driessche, P. (2013). Global stability of infectious disease models using Lyapunov functions. *Faculty Bibliography 2010s*, 4700.

Guo, H., & Li, M. (2006). Global stability in a mathematical model of tuberculosis. *The Canadian Applied Mathematics Quarterly*, *14*.

Bentaleb, D., Amine, S., & Khatar, Z. (2019). Global stability of SEIR model using Lyapunov function method. *Journal of Theoretical and Applied Information Technology*, *97*(16).

Pontryagin, L. S. (1987). *Mathematical Theory of Optimal Processes*. Routledge.